BANK OF ENGLAND

Staff Working Paper No. 990

Decomposing the drivers of Global *R**

Ambrogio Cesa-Bianchi, Richard Harrison and Rana Sajedi

July 2022

BANK OF ENGLAND

Staff Working Paper No. 990
Decomposing the drivers of Global *R**

Ambrogio Cesa-Bianchi,[1] Richard Harrison[2] and Rana Sajedi[3]

Abstract

We use a structural overlapping-generations model to quantify the effects of five exogenous forces that drive the global trend equilibrium real interest rate, Global *R**. We use data for 31 countries to extract the global trend components of the five drivers and to derive an empirical estimate of Global *R**, which we use to calibrate the model. We design a recursive simulation method in which beliefs about the future path of the drivers are updated gradually. In our simulation, Global *R** rises from the mid-1950s to the mid-1970s, declining steadily thereafter. The decline is driven predominantly by slowing productivity growth and increasing longevity.

Key words: Equilibrium interest rates, structural change, demographics.

JEL classification: E22, E43, J11.

(1) Bank of England, CEPR and CfM. Email: ambrogio.cesa-bianchi@bankofengland.co.uk
(2) Bank of England and CfM. Email: richard.harrison@bankofengland.co.uk
(3) Bank of England and CfM. Email: rana.sajedi@bankofengland.co.uk

The views expressed in this paper are those of the authors, and not necessarily those of the Bank of England or its committees. We are grateful to Caroline Butler and Veronica Veggente, who provided outstanding research assistance, and to Andrea Ferrero, Pierre-Olivier Gourinchas, Thomas Laubach, Nick McLaren, Gregory Thwaites, and conference participants at RES 2019, for useful comments and suggestions.

The Bank's working paper series can be found at www.bankofengland.co.uk/working-paper/staff-working-papers

Bank of England, Threadneedle Street, London, EC2R 8AH
Email enquiries@bankofengland.co.uk

ISSN 1749-9135 (on-line)

1 Introduction

In almost every country in the world, the real returns on long-term government bonds are lower than they were 40 years ago. The observation that real interest rates have fallen in a similar way across many countries suggests that common global forces may be at play. If so, what are these forces, and which have been most important for driving long-run real interest rates? The answers to these questions have potentially far-reaching implications for the design and implementation of macroeconomic policy frameworks around the world.

In the long run, when capital can move freely across countries, standard macroeconomic theory implies that there exists a single global equilibrium real interest rate, which we call 'Global R^*'. The level of Global R^* is determined by the global supply and demand for capital. This approach therefore implies that the common decline in long-run interest rates across the world reflects trends in factors that drive global wealth and capital accumulation. In this paper, we use this conceptual framework for Global R^* to uncover the key global drivers of equilibrium interest rates since 1950.

We study the determinants of Global R^* by integrating structural modelling and reduced-form empirical techniques. We build a structural model of the world economy, which includes five observable drivers of R^*: productivity growth, population growth, longevity, the relative price of capital and government debt. Using data for a panel of 31 countries from 1950 to 2015, we derive the common global trend in each driver, as well as a reduced-form empirical estimate of Global R^*—both of which are used to guide the calibration and simulation of the model.

The structural model treats the world as a single large (closed) economy, populated by overlapping generations of finitely-lived households. The model is calibrated so that each period corresponds to 5 years, thereby capturing the effects of slow-moving trends and abstracting from business-cycle fluctuations. Accordingly, we extract from our panel data the low-frequency common component of each series of interest. We use our empirical estimate of Global R^* to anchor the initial level of the real interest rate at the start of our sample (in 1951-55) and use the structural model to simulate the path of the interest rate in response to the observed dynamics of the global drivers over the subsequent sixty years.

The model simulations are constructed using a novel recursive approach that captures slow-moving beliefs about long-term trends, consistent with evidence of persistent errors in forecast-

ing trend productivity and demographics. This method incorporates the effect of changes in the trend components of the drivers on beliefs about their future evolution, which is important for our results because the simulations span sixty years of substantial structural change.

Our simulations show that Global R^* rises from 1.25% in the mid-1950s to around 2.75% in the mid-1970s. Thereafter, Global R^* declines steadily, reaching -0.25% at the end of our sample in 2015. In the early part of our sample, higher productivity growth and population growth (the 'baby boom') raise Global R^*. The subsequent decline is predominantly driven by falling productivity growth and increased longevity. The relative price of capital has only a modest effect on the equilibrium real interest rate and, at a global level, movements in trend government debt are not sufficient to have a material impact on R^*.

Our structural model implies a path for Global R^* that is remarkably consistent with the estimates from the reduced-form empirical approach. Furthermore, by identifying the underlying forces that account for these dynamics, the results of the structural model suggest that, without a substantial reversal in the trends in productivity growth or longevity, Global R^* is likely to remain low.

Our paper is related to several strands of the literature. We move beyond existing work using structural models by considering a range of potential drivers of R^*, at the global level, within a single framework.[1] Eggertsson et al. (2019) undertake an exercise that is similar to ours, analysing a similar set of drivers within a structural model, but they focus on the United States as a closed economy, thereby abstracting from the global nature of many of these trends. Conversely, studies of global equilibrium real interest rates have typically focused on a narrower subset of drivers. For example, Lisack et al. (2021) focus solely on the role of demographic drivers across advanced economies. Similarly, while Rachel and Summers (2019) also emphasise the importance of the global dimension of R^*, their analysis focuses on the role of various fiscal policy instruments.

Our analysis complements and extends existing empirical estimates of global equilibrium real interest rates. Most closely related to this paper are the estimates of R^* at a global level in Del Negro et al. (2019) and Kiley (2020), who extract a common trend from their panel of 7 and 13 countries, respectively. Their estimates suggest that Global R^* fell by around 3

[1] An early contribution to the literature on the structural determinants of global real interest rates is Rachel and Smith (2017), though they combine the results of several alternative models to form their estimates.

percentage points between 1980 and 2015. Our empirical estimate, which applies a variant of the Del Negro et al. (2019) approach to our panel of 31 countries, suggests a slightly smaller decline, of approximately 2.25%, over this period.

Our results are also related to estimates of equilibrium real interest rates for individual countries. Many existing studies use closed-economy semi-structural models to estimate a higher frequency concept of the equilibrium real interest rate: the real interest rate that stabilises output at potential and inflation at target (see, for example, Laubach and Williams, 2003; Holston et al., 2017). That framework therefore implies that the 'short-term' equilibrium interest rate is typically determined by cyclical domestic shocks. Our approach, which aims to identify the role of longer-term global trends, purposefully abstracts from shorter-term deviations of an individual economy's real interest rate from Global R^*, and hence the effects of shocks on domestic equilibrium rates over shorter horizons. Nevertheless, over longer horizons, Global R^* acts as an anchor for domestic equilibrium real interest rates in open economies, so that estimates of Global R^* are important ingredients for longer-term analysis, including the design of policy frameworks.

The rest of the paper is organised as follows. Section 2 describes our structural model, while Section 3 describes how we obtain the empirical measures of the global trend in the key model drivers. Section 4 explains the calibration and the details of the recursive simulation method. Section 5 describes the results of the model simulations, including a decomposition into the contributions from each driver. Section 6 examines the robustness of the baseline results to alternative assumptions and provides a discussion of several potential drivers that are not included in the model. Section 7 concludes.

2 The Overlapping-Generations Model

This section provides an overview of the overlapping-generations (OLG) model used for our structural exploration of the global equilibrium real interest rate. We focus here on the decision problems of the agents in the model, with a full derivation presented in Appendix A.

2.1 Households

A household born in period t lives for a maximum of T periods, with $\Pi_{t,\tau}$ denoting the unconditional survival probability at age τ (i.e., the fraction of the generation born in period t that will survive until age τ), with $\Pi_{t,1} = 1$ and $\Pi_{t,T+1} = 0$.

Households have access to an asset, a, which pays a net real interest rate, r. At each age, τ, the household supplies ρ_τ units of labour inelastically, for wage $w_{t+\tau-1}$.[2] The household receives a stream of non-labour income, $\varpi_{t,\tau}$, which they treat as exogenous.

Households maximise their expected lifetime utility, given by:

$$U_t = \sum_{\tau=1}^{T} \beta_\tau \Pi_{t,\tau} \frac{c_{t,\tau}^{1-\theta}}{1-\theta},$$

subject to a budget constraint in each period:

$$c_{t,\tau} = \rho_\tau w_{t+\tau-1} + (1 + r_{t+\tau-2}) a_{t,\tau-1} - a_{t,\tau} + \varpi_{t,\tau},$$

with $a_{t,0} = a_{t,T} = 0$, so that households are born with no assets and do not leave any bequests at the end of their lives.[3]

This optimisation problem yields the familiar Euler equations:

$$1 = \frac{\beta_{\tau+1}}{\beta_\tau} \frac{\Pi_{t,\tau+1}}{\Pi_{t,\tau}} \left(\frac{c_{t,\tau+1}}{c_{t,\tau}} \right)^{-\theta} (1 + r_{t+\tau-1}) \qquad \text{for } \tau = 1 \ldots T-1.$$

2.2 Firms

A monopolistic retailer buys Y_t units of an intermediate good and sells it with a net mark-up, μ, over marginal cost. Normalising the price of the final good to 1, this means the relative price of the intermediate good is given by $1/(1+\mu)$. The aggregate profit of the retailer, given by:

$$\Xi_t = \frac{\mu}{1+\mu} Y_t,$$

[2] Note that $t + \tau - 1$ is the period in which the generation born in period t is aged τ.

[3] Households that do not reach age T will leave accidental bequests, which will be incorporated in non-labour income.

is distributed to the households. The intermediate good is produced with capital, K, brought forward from the previous period, and labour, L, using a CES production function:

$$Y_t = \left(\alpha K_{t-1}^{\frac{\sigma-1}{\sigma}} + (1-\alpha)(E_t L_t)^{\frac{\sigma-1}{\sigma}} \right)^{\frac{\sigma}{\sigma-1}} ,$$

where E_t is a labour-augmenting technological process with net growth rate e_t.

The intermediate-good-producing firm's profit maximisation can be written as:

$$\max_{K_t, L_t} \quad \frac{1}{1+\mu} Y_t - \left(r_t^k p_t^k K_{t-1} + w_t L_t \right) ,$$

where p^k is the relative price of capital, r^k is the rental rate of capital, and w is the wage per units of labour. This gives the first-order conditions:

$$\begin{aligned} r_t^k &= \frac{1}{1+\mu} \alpha \frac{1}{p_t^k} \left(\frac{Y_t}{K_{t-1}} \right)^{\frac{1}{\sigma}} , \\ w_t &= \frac{1}{1+\mu} (1-\alpha) E_t \left(\frac{Y_t}{L_t} \right)^{\frac{1}{\sigma}} . \end{aligned}$$

2.3 Government

The government issues a stock of debt, G, on which it pays interest, r. This interest payment is financed by lump-sum taxes levied on households, $\mathcal{T}$. Hence the government budget constraint is given by:

$$G_t = (1 + r_{t-1}) G_{t-1} - \mathcal{T}_t .$$

2.4 Financial Intermediary

At the end of each period, a financial intermediary takes the aggregate assets of the households, promising a net return of r_t per unit in the next period. They turn these assets, net of government bonds, into the capital good, with a technology that transforms 1 unit of the consumption good into p_t^k units of capital goods. The intermediary stores these capital goods and makes them available for production in the next period. As above, K_t denotes the capital stock available for production in period $t+1$. Hence the financial intermediary must repay $(1 + r_t) p_t^k K_t$ to the households in period $t+1$.

To pay this return, the intermediary rents the capital stock to the firm. The firm pays the rental cost, $r^k_{t+1}K_t$, and returns the un-depreciated capital stock, $(1-\delta)K_t$, to the intermediary. Furthermore, if the relative price of capital goods changes, the intermediary earns this revenue at relative price p^k_{t+1}. Hence the profit of the intermediary, denominated in terms of the consumption goods, is:

$$\begin{aligned}\Phi^d_{t+1} &= p^k_{t+1}\left(r^k_{t+1}K_t + (1-\delta)K_t\right) - (1+r_t)p^k_t K_t \\ &= \left((1+r^k_{t+1}-\delta)\frac{p^k_{t+1}}{p^k_t} - (1+r_t)\right)p^k_t K_t \\ &= \phi^d p^k_t K_t\,,\end{aligned}$$

where we have denoted by ϕ^d the profit per unit of capital, which we assume to be fixed. In other words, ϕ^d represents the fixed spread between the return on capital and the risk-free rate:

$$1 + r_t = (1 + r^k_{t+1} - \delta)\frac{p^k_{t+1}}{p^k_t} - \phi^d\,.$$

These profits are treated as a resource cost to the economy, which can also be viewed as an additional cost that the financial intermediary is paying, such as the cost of storing capital.

2.5 Aggregation

We complete the description of the model by defining some aggregate concepts.

Population growth. Let N_t be the size of the cohort born at time t, and $n_t \equiv \frac{N_t - N_{t-1}}{N_{t-1}}$ the net growth rate of consecutive cohorts.

Labour. Total labour supply is given by:

$$L_t = \sum_{\tau=1}^{T} \rho_\tau \Pi_{t,\tau} N_{t-\tau+1}\,.$$

Asset markets. The aggregate assets of the household are either used to buy the stock of government bonds, or turned into capital by the financial intermediary:

$$p_t^k K_t + G_t = \sum_{\tau=1}^{T} N_{t-\tau+1} \Pi_{t,\tau} a_{t,\tau} \, .$$

Households that die between periods leave their assets, along with the return, as accidental bequests. Aggregate accidental bequests are given by:

$$\mathcal{B}_t \;\; = \;\; (1 + r_{t-1}) \sum_{\tau=1}^{T} (1 - \frac{\Pi_{t,\tau+1}}{\Pi_{t-1,\tau}}) \Pi_{t-1,\tau} N_{t-\tau} a_{t-1,\tau} \, .$$

Non-labour income. The non-labour income of the household, ϖ, comprises of the monopolistic profit of the retailer, the accidental bequests, less the lump-sum taxes paid to the government. These objects have thusfar been defined as aggregates in each period. To account for how they are distributed among the different generations, we introduce the parameters $\{\xi_\tau, \mathfrak{b}_\tau, \mathfrak{t}_\tau\}_{\tau=1}^{T}$ such that the total non-labour income of each generation τ can be written as:

$$\Pi_{t,\tau} N_{t-\tau+1} \varpi_{t,\tau} = \xi_\tau \Xi_t + \mathfrak{b}_\tau \mathcal{B}_t - \mathfrak{t}_\tau \mathcal{T}_t \, ,$$

with $\sum_{\tau=1}^{T} \xi_\tau \; = \sum_{\tau=1}^{T} \mathfrak{b}_\tau = \sum_{\tau=1}^{T} \mathfrak{t}_\tau = 1$.

2.6 The Drivers

This model has five exogenous processes, which we refer to as the 'drivers', that determine equilibrium allocations and prices, including the interest rate, r_t. These are: (i) e_t, the growth rate of the labour-augmenting technology; (ii) n_t, the population growth rate; (iii) $\Pi_{t,\tau}$ for $\tau = 2, ...T$, the survival probabilities at each age; (iv) $GY_t \equiv G_t/Y_t$, the government debt to GDP ratio; and (v) p_t^k, the relative price of capital goods. In what follows, we denote the vector of the drivers in each point in time as $d_t \equiv \left[e_t, \, n_t, \, \Pi_{t,2}, \ldots, \Pi_{t,T}, \, GY_t, \, p_t^k\right]'$.

3 Drivers of Global R^*

This section describes the construction of observable proxies for the exogenous processes in d_t, which drive changes in the global equilibrium real interest rate, Global R^*. Our starting

point is the notion that the drivers of Global R^* can be recovered as common factors from a large panel of countries. Del Negro et al. (2019) show that, according to standard asset-pricing theory, a no-arbitrage condition in the long run implies a factor structure in the trends of real interest rates across countries. Following this insight, we compile a large data set comprising 31 'high-income' countries, with observable proxies for the exogenous processes in the model.[4]

Specifically, for three of our drivers, we obtain data on the stock of government debt from IMF Global Debt Database, the relative price of capital goods from the Penn World Tables (PWT), and the growth rate of the labour-augmenting technology from Ziesemer (2021). The data are at annual frequency and cover the period from 1951 to 2015.[5] Appendix C provides additional details on the sources of the data.

To map the data to the model, we proceed in three steps. First, we extract a common (or 'global') component from country-specific data.[6] We approximate the global component by exploiting our large cross-section of countries and using cross-sectional (weighted) averages. As shown in Pesaran (2006), when the number of cross-sectional units is large, cross-sectional averages can approximate common factors in a similar way to principal components or other more sophisticated techniques.[7] For the calculation of weighted averages we use time-varying GDP weights from PWT (expenditure-side real GDP at current PPPs, in mil. 2017US$).

Second, given our focus on slow-moving dynamics, we abstract from cyclical fluctuations and extract the low-frequency movements from the estimated global factors using an HP filter, with a smoothing parameter of $\lambda = 1,000$. This choice is based on prior beliefs about the volatility of the trend component of the drivers. Lower values of the smoothing parameter, as commonly employed to recover the *cyclical* component of annual data, imply implausible values for the volatility of shocks to the trend.[8]

Third, we adjust the data to match the calibration of the model, in which each discrete time

[4] We define a country as high income when its output per capita (measured as expenditure-side real GDP at current PPPs in mil. 2011US$ divided by total population) in 2014 is above 25,000$. See Appendix C for details.

[5] We explicitly exclude 2020 to avoid the large movements induced by the Covid-19 shock.

[6] We do this for each of the observables described above, with the exception of population growth and cohort-specific survival probabilities for which we obtain aggregate figures from the UN World Population Prospects. See details below.

[7] While a large cross-section is the key assumption to obtain this result, some additional regularity conditions on the weights and the factor loadings are also needed. See Pesaran (2006).

[8] Ideally, the choice of λ should be adjusted so that it reflects prior knowledge on the length of the cycle. However, the smoothing parameter also affects the volatility of the trend – a consequence of the fact that the HP filter does not contain an explicit model of both the trend and the cycle. As a result, there is also a link between the prior for the variance of trend innovations and the HP smoothing parameter. The sensitivity tests in Section 6 consider alternative assumptions for λ.

period is assumed to be 5 years. We employ the convention that the first period in the model simulations corresponds to 1951-1955 in the data, the second period corresponds to 1956-1960, and so on. The annual growth rate of the labour-augmenting technology, e_t, is compounded to compute a 5-year growth rate. For government debt to GDP, GY_t, we take the value of the annual debt to GDP at the end of each 5-year period in the data, and divide it by 5 to obtain the 5-year ratio, consistent with the end-of-period definition in the model.[9] For the relative price of capital, p_t^k, we take an average of the annual values within each 5-year period in the data.

The two demographic drivers, population growth and survival probabilities, are treated separately. We obtain the underlying data on population numbers by age group from the UN World Population Prospects, which provides data at 5-year frequency for a group of high-income economies that is comparable to our baseline sample of 31 countries. This gives us the total number of people in our group of countries, in each 5-year age cohort, at the end of each 5-year period from 1955-2015. In line with the calibration of the model, we consider the age groups starting from 20-24 years old up to 85-89 years old. From this raw population data, we calculate n_t as the growth rate of consecutive 20-24 year old cohorts, and $\Pi_{\tau,t}$ as the ex-post change in the size of a given cohort over time.

We do not detrend these series since demographic trends are inherently slow moving, and therefore only relevant for long-run concepts of equilibrium interest rates. That is, short-run changes in population growth and survival probabilities are unlikely to have a material impact on equilibrium interest rates. We therefore assume that the observed evolution of population growth and cohort-specific survival probabilities coincide with the trend.

Figure 1 plots the drivers of Global R^* derived from the procedure described above. The yellow line plots the common factors obtained by means of cross-sectional weighted averages and, where relevant, the blue line with circles plots the trend component obtained with the HP filter. For readability, the drivers are re-scaled to be in yearly space.[10]

The figure highlights a few secular trends that are common to the large group of economies we consider: (i) productivity has been declining steadily since the mid-1960s; (ii) after falling in

[9] We could adjust for the cumulative GDP over 5 years instead, but this would not affect the final trend path that we estimate.

[10] For the labour-augmenting technological growth and population growth, we plot the average growth rate over each 5-year period, for government debt over GDP we plot the stock of government debt over annual GDP at the end of the 5-year period. The relative price of capital requires no re-scaling.

Figure 1 Global trends in the five drivers

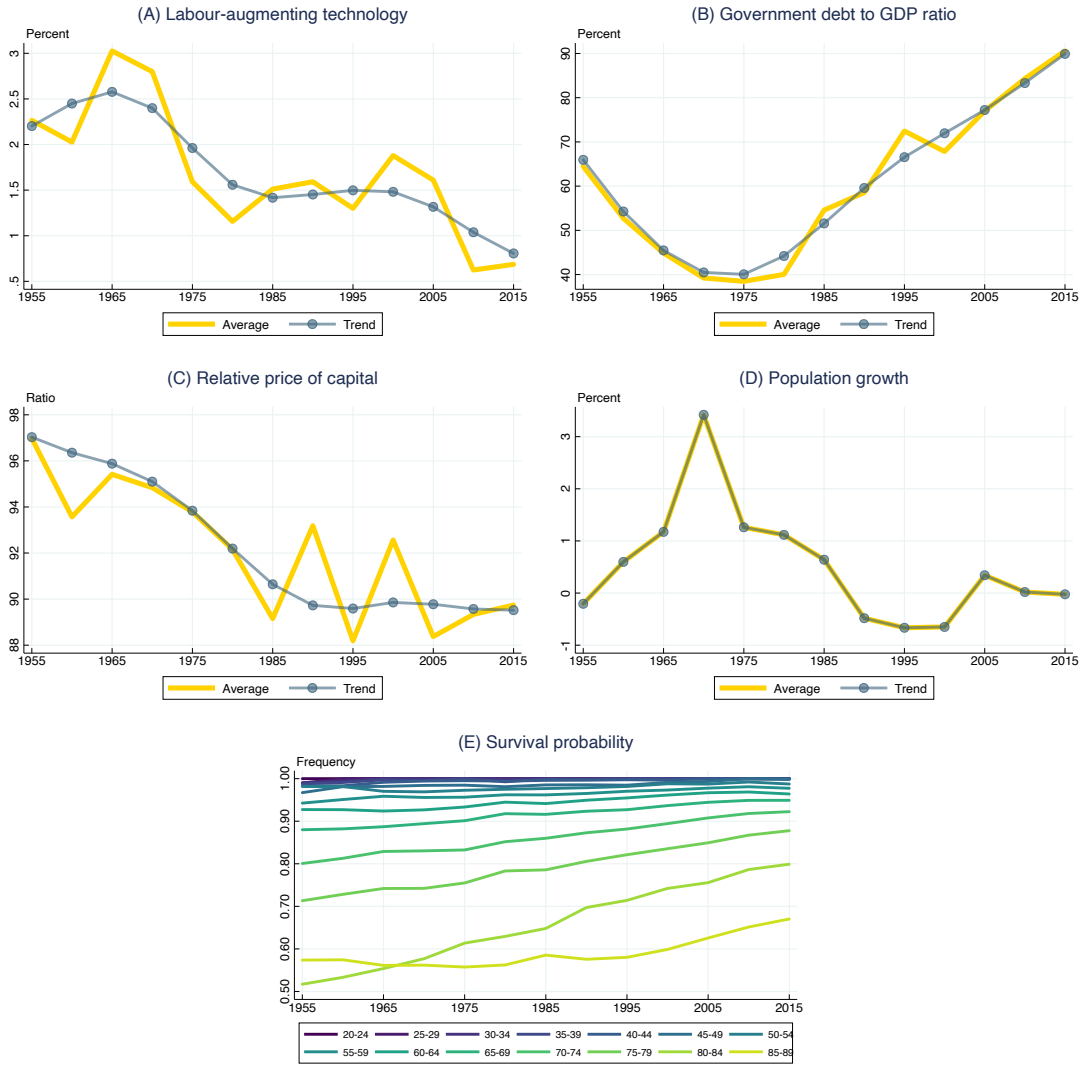

NOTE. The figure plots the observable proxies for the exogenous processes that drive changes in the global equilibrium real interest rate in the structural model. In panels (A) to (D), the yellow line plots the common factors obtained with cross-sectional weighted averages of the observables, while the blue line with circles plots the trend component obtained with the HP filter. In panel (E) each line plots the evolution over time of the survival probability for each cohort. Sample period: five-year periods from 1955 to 2015, where '1955' corresponds to the period 1951-1955.

the first part of the sample, government debt has been trending upwards since the 1970s; (iii) the relative price of capital has fallen steadily since 1955; (iv) after peaking in 1960, population growth has slowed down significantly, remaining roughly constant since the 1990s; (v) longevity, as measured by the survival probability, has dramatically increased for most cohorts, and in particular for those aged over 65.

These secular trends will have implications for the equilibrium real interest rate in our

structural model. In the next section, we will explain how we feed these estimated paths for the drivers through the model simulations, to obtain a model-implied path for Global R^*.

4 Calibration & Solution Method

This section describes our approach to calibrating and simulating the model. For ease of exposition, we first describe the recursive simulation method for a given set of parameter values, before turning to the selection of key parameter values. Further details are provided in Appendix B.

4.1 Recursive simulation method

Let x_t denote the vector of all endogenous variables in the model in each period t, and d_t the vector of (exogenous) drivers. The model described in Section 2 is a function, f, such that, in each period:

$$f\left(x_{t-1}, x_t, x_{t+1}; d_t\right) = 0\,, \tag{1}$$

where d_t is the vector of trend estimates of the drivers as described in Section 3.

Our objective is to explore the role of the drivers, d, in determining the behaviour of one of the elements of x, namely the equilibrium real interest rate, over our sample, $1955 - 2015$, which we will denote by $t = 1, \ldots, H$.[11]

Most of the existing literature studying the secular trend in the equilibrium real interest rate computes the equilibrium sequence $\{x_t\}_{t=1}^{H}$ using an assumption of perfect foresight. In other words, these studies assume that the entire path of $\{d_t\}_{t=0}^{\infty}$ is known from $t = 0$. This is an extreme assumption. The sixty-year sample we consider contains dramatic changes in the drivers over time, as shown in Figure 1, and, importantly, these changes were not entirely foreseen.[12] We therefore extend our simulation method to account for how expectations of future developments evolved over time.

To study the slow-moving determinants of the equilibrium real interest rate over time, and capture the gradual updating of beliefs, we assume that agents use a random walk forecasting

[11] We can also produce forecasts $x_{H+j}, j = 1, \ldots,$ though that is not the focus of the paper.

[12] See, for example, Dowd et al. (2010) and and Edge et al. (2007) on forecast errors for demographics and productivity respectively.

model for the drivers. Specifically, expectations in period t are assumed to satisfy:

$$d_{t+i|t} = d_t \quad , \quad i = 0, \ldots, \infty \, .$$

This approach implies that in each period the current values of the drivers are expected to prevail forever, so that the economy is expected to transition to a steady state defined by those values of the drivers. So, in period t, the steady state that agents expect the economy to converge to, denoted by x_t^{ss}, is found by solving:

$$f\left(x_t^{ss}, x_t^{ss}, x_t^{ss}; d_t\right) = 0 \, .$$

This equation defines an implicit function relating the drivers to the steady-state values of the endogenous variables:

$$x_t^{ss} = g\left(d_t\right) \tag{2}$$

Thus, the period t solution is found by solving for the deterministic transition path to x_t^{ss}, conditional on the vector of endogenous variables determined in period $t-1$ (i.e., x_{t-1}). The resulting solution for period t, x_t, then becomes the initial condition for the subsequent period $t+1$ solution. In other words, the recursive simulation consists of a sequence of projections that account for the evolving information set of agents in the model.

Formally, the recursive simulation is constructed as follows:

1. Set an initial condition x_0.

2. For each period $t = 1, \ldots, H$, solve (2) to find x_t^{ss}, i.e., the steady state of the endogenous variables in the model assuming that the drivers stay at their period t value forever.

3. For period $t = 1$, solve the full deterministic transition path from x_0 to x_1^{ss} using the dynamic model, (1), under the assumption that $d_{t+i} = d_1$ for $i > 0$. Record the period 1 solution of this transition path as x_1.

4. For each period $t = 2, \ldots, H$, solve the full transition path from x_{t-1} to x_t^{ss} using the dynamic model, (1), under the assumption that $d_{t+i} = d_t$ for $i > 0$. Record the solution for the first period of this transition as x_t, which will then also become the initial condition for period $t+1$.

The rest of this section describes how the parameters are set, and how the initial condition x_0 is chosen.

4.2 Calibration

The above description of the model and simulation method abstracted from the issue of setting parameter values.

Each period in the model lasts for five years. Based on the demographic data described in Section 3, we assume that there are $T = 14$ cohorts, with the youngest cohort consisting of households aged 20-24 and the oldest consisting of those aged 85-89.

We set values for a subset of parameters based on values used in previous studies, as shown in Table 1. In particular, the values for α, σ, δ and θ follow Lisack et al. (2021) and references therein. The mark-up parameter is set to 0.1, broadly in line with the global estimates for 1980 (roughly the middle of our sample) presented by De Loecker and Eeckhout (2018). The capital return spread, ϕ^d, is consistent with an average 2.7% annual spread between the return on capital and the safe real rate.[13]

Table 1 Baseline parameter values

Parameter	Description	Value
α	Weight of capital in production function	0.33
σ	Elasticity of substitution in production function	0.70
δ	Capital depreciation rate	0.21
θ	Intertemporal elasticity of substitution	1.00
μ	Firms' price mark-up	0.10
ϕ^d	Capital return spread	0.22

One of the key model parameters is the vector of discount factors, $\{\beta_\tau\}_{\tau=1}^{T}$. A common approach in models with infinitely-lived agents is to use information about the steady-state real interest rate to calibrate the (single) discount factor. As we are modelling dynamic changes in the real interest rate, this approach is not directly applicable here. Instead, in a similar spirit, we choose the discount factors so that the real interest rate and distribution of asset holdings across households ($\{a_\tau\}_{\tau=1}^{T}$) in the 1955 steady state (x_1^{ss}) match two targets. The target for the 1955 steady-state real interest rate is the average of an empirical estimate of Global R^* over

[13] The average annual spread is estimated by taking the difference between the average product of capital from Caballero et al. (2017) and the long-term real interest rate in Del Negro et al. (2019) using US data.

the period 1900–1950, based on the same 31 countries that were used to estimate the drivers. This estimate of Global R^* is described in Appendix D, and discussed further in Section 5.2 below. The target for the asset distribution is based on evidence on the life-cycle distribution of wealth in Lisack et al. (2021) and Auclert et al. (2021). Appendix B.2 provides further details.

The remaining parameters in the model are the cohort-specific labour supply, ρ_τ, and the parameters that govern the distribution of bequests, taxes and monopolistic profits among the cohorts. For the latter, we assume that in all cases these are distributed equally among working-age cohorts only. In other words we assume $\xi_\tau = \mathfrak{b}_\tau = \mathfrak{t}_\tau = 1/9$ for $\tau = 1, \ldots, 9$ and $\xi_\tau = \mathfrak{b}_\tau = \mathfrak{t}_\tau = 0$ for $\tau = 10, \ldots, 14$. We calibrate ρ_τ in line with the evidence on the life-cycle profile of labour force participation.[14]

4.3 Initial conditions

The first step in the recursive simulation is to choose values for the initial conditions x_0. The approach is described in detail in Appendix B.3. However, we emphasise two important aspects of the approach. First, we use as much data as possible for period $t = 0$ (i.e., 1946-1950). Where data is not directly available we combine steady-state model relationships with other data to impute consistent values for the missing variables. Second, because population data *is* available, initialising the model using the observed age structure of the population ensures that we match population dynamics for all cohorts in all subsequent periods.

5 Results

This section presents the results from the model simulation approach described above. We first compare our recursive simulation with a simulation based on 'perfect foresight', demonstrating the impact of the assumptions about the evolution of expectations of the drivers. We then compare the model simulation with an empirical estimate from a version of the Del Negro et al. (2019) model using our expanded data set. Finally, we present a decomposition of our simulation to uncover the importance of each driver in determining the path of Global R^*.

As noted above, each time period in the model lasts for five years, so that the one-period

[14] The precise calibration is based on US data, where we have sufficient granularity across cohorts, but the evidence is in line with other countries. Appendix C.2 provides full details.

interest rate in the model is a five-year rate of return. For ease of exposition, all interest rates are presented as annualised (i.e., annual equivalent) percentages.[15]

5.1 Recursive Simulation Results and Properties

Figure 2 presents our baseline recursive simulation alongside a simulation based on the more standard assumption of perfect foresight. The perfect-foresight variant assumes agents fully anticipate the future paths of all of the drivers from the start of the simulations.

Figure 2 Recursive simulation versus perfect foresight transition

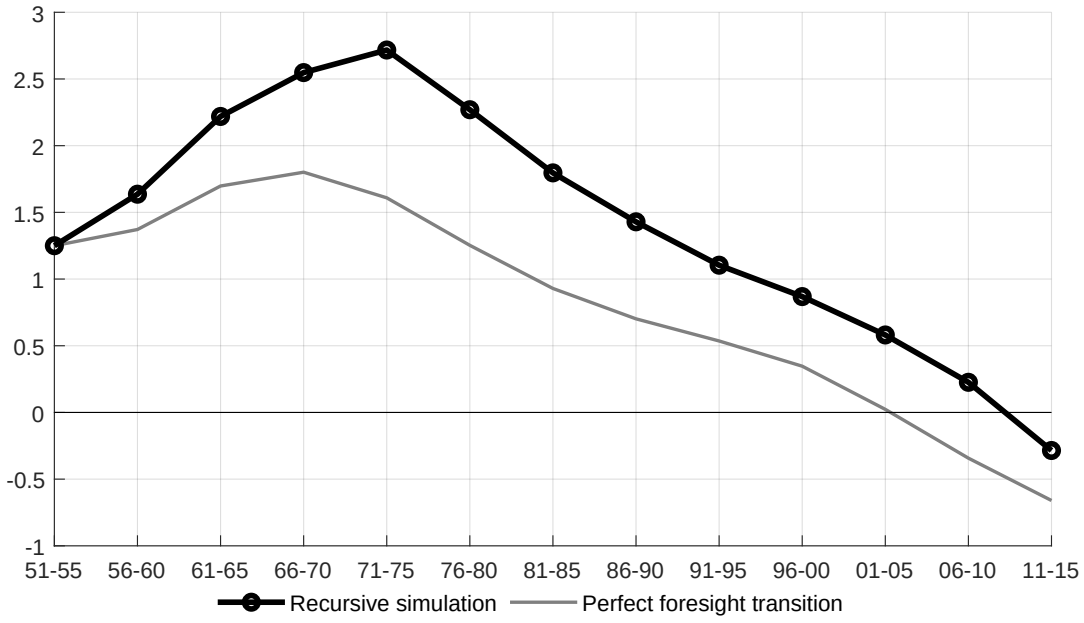

NOTE. The black line with circles is the baseline simulation generated by our recursive simulation method. The grey line is the result of a simulation in which the full paths of all drivers are fully anticipated at the start of the simulation. All interest rates are expressed as annualised percentage rates, corresponding to the five-year real interest rates for the periods indicated by x-axis labels.

Our recursive simulation implies that Global R^* rises from the mid-1950s to the mid-1970s before declining steadily until the end of our sample in 2015. In contrast, when the paths of the drivers are fully anticipated (grey line), the peak in Global R^* is smaller and occurs earlier. Assuming that agents have perfect foresight implies that they observe the evolution of the drivers until the latter part of our sample (e.g., 2011–2015) at the very start of the simulation (1951–1955). The value of the drivers in the distant future exerts a downward force on equilibrium real interest rates in the early part of the sample because agents foresee the

[15]The five-year real interest rate in the model is r, and the annualised equivalent is $100 \times \left((1+r)^{\frac{1}{5}} - 1\right)$.

forces that will eventually drive the economy to a steady state in which the real interest rate will be very low.[16]

We regard the assumptions underpinning the recursive approach in our baseline simulation as more plausible than the assumption that agents foresaw the entire evolution of the drivers from the mid-1950s. While this perspective may be open to debate for some of the drivers, there is ample evidence that key elements of the demographic transition in the twentieth century were not foreseen (see, for example, Booth, 2006).

Figure 2 also reveals that both the baseline recursive simulation and the perfect foresight variant imply that Global R^* drops below zero towards the end of the sample. We note that the presence of imperfectly-competitive producers in our model allows the equilibrium real interest rate to be negative, even in the long run (see the discussion in Eggertsson et al., 2019).

Figure 3 Recursive simulation paths

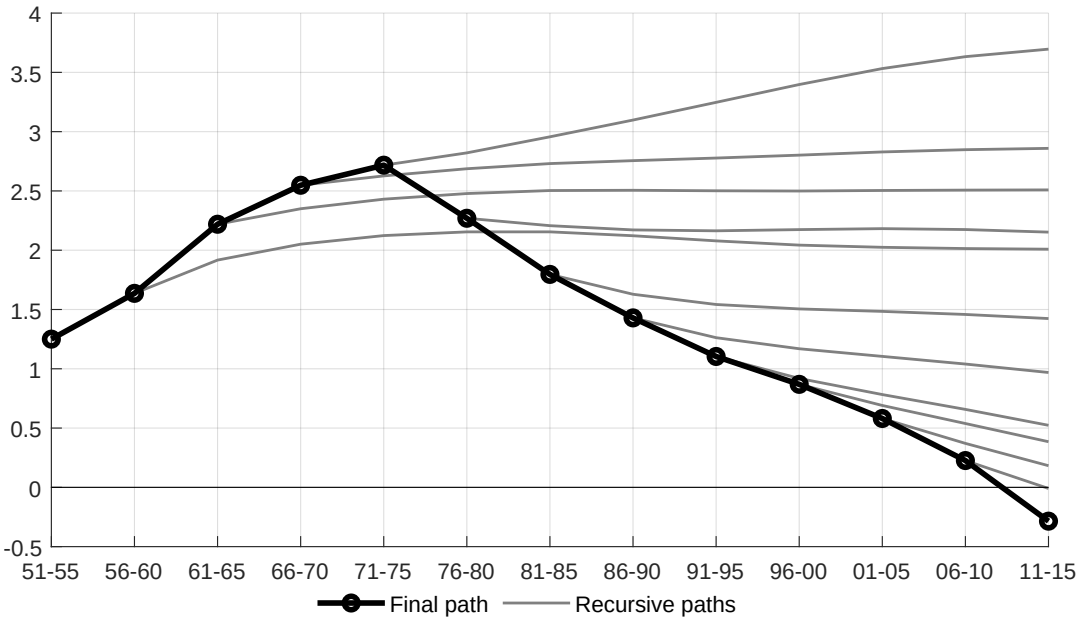

NOTE. The black line with circles is the baseline estimate formed by taking the first period of each recursive simulation, and the grey lines show the sequence of transitions towards steady state from each recursive simulation. All interest rates are expressed as annualised percentage rates, corresponding to the five-year real interest rates for the periods indicated by x-axis labels.

Figure 3 sheds further light on the importance of agents' recursive updating of their beliefs, by plotting the full results of each simulation within the recursion alongside the final estimate. In particular, the grey lines show the transition towards steady state, which is constructed in

[16] We discuss these forces in detail in Section 5.3 below.

each period using the steps described in Section 4.1. The black line is the baseline estimate, formed by taking the sequence of solutions for the first period of each recursive simulation.

The figure reveals that revisions to the expected paths of the drivers initially led to expectations of persistent increases in Global R^*, though the subsequent evolution of the drivers pushed up Global R^* by more than initially expected. That is, in the early part of the simulation, the sequence of recursive paths (grey lines) moved upwards over time. From the mid-1970s, when the baseline estimate of Global R^* peaks, the expected paths of real rates moved persistently downwards. So from this point on, movements in the drivers led to a sequence of downward revisions in beliefs about the future prospects for Global R^*.[17]

5.2 Comparison with an Empirical Estimate

In this section, we compare the simulated path for Global R^* from the OLG-model simulation with an empirical estimate of the global trend in real interest rates. As discussed above, the empirical estimate is also used to provide an anchor for the OLG simulation. In particular, as described in Sections 4.2 and 4.3, we calibrate the initial steady state to be consistent with the historical average of the series, and also set the initial condition for the recursive simulation in line with the empirical estimate.

To derive this empirical estimate, we use a VAR with common trends, closely following the approach of Del Negro et al. (2019), to model the joint dynamics of short-term interest rates, long-term interest rates, and inflation, using annual data from 1900 to 2015. The key innovation is to estimate the model using data from our panel of 31 economies.[18] The model is cast in state-space form and estimated with Bayesian methods. The details of the model (including the general representation, derivation of the baseline specification, priors, and initial conditions) are reported in Appendix D.

Figure 4 shows the baseline OLG-model simulation alongside this empirical estimate. We plot the OLG estimate as five-year lines, to emphasise that the model determines the interest rate for successive five-year periods, though (as in all other charts) we plot the OLG results as an annualised percentage rate. The empirical estimate of Global R^* was relatively stable at

[17] As Figure 3 suggests, beyond 2015 the simulated path of Global R^* falls further as the world economy continues to adjust to the steady state consistent with 2011-2015 beliefs about the long-run paths of the drivers.

[18] Figure C.2 in the Appendix reports the raw series for the short-term real interest rates for each country, computed as the nominal short-term interest rate minus the realised inflation rate.

around 2.25% in the first part of the sample, between 1900 and 1930. After falling to 1.25% around the second world war, the empirical estimate rose again between 1950 and 1980, reaching a peak of around 2.5%. Since the 1980s, Global R^* has been on a downward path, approaching 0% in recent years.[19]

Figure 4 Baseline OLG simulation and empirical estimate

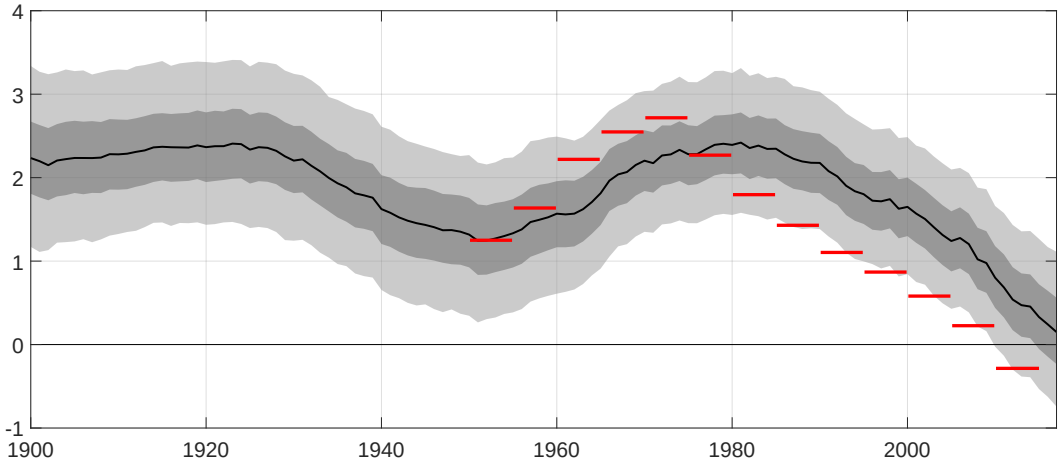

NOTE. The solid black line is the posterior median of the empirical estimate of Global R^* presented in Appendix D and the shaded areas show the 68 and 95 percent posterior intervals. The red lines show the baseline path for the real interest rate generated by the OLG model, as shown in Figure 2. All interest rates are annualised percentage rates.

As described in Section 4.3, the OLG and empirical estimates are very close at the start of the simulation by construction given our initialisation approach. Thereafter the OLG estimate rises more quickly than the median empirical estimate, peaking slightly earlier. The peak real rate of around 2.5% for 1971–1975 is broadly in line with the empirical estimate at that time, lying slightly above the 68% posterior interval. Beyond the peak, the real rate from the OLG model simulation falls more quickly than the empirical estimate, reaching −0.25% by the end of the sample.

5.3 Decomposing the Drivers of Global R^*

We now turn to the decomposition of the baseline path for Global R^* into the contributions of individual drivers. Figure 5 shows the baseline simulation, and the decomposition, relative to

[19] Despite the different approaches and samples of countries, alternative empirical estimates of Global R^* from the recent literature show similar patterns, especially since the 1980s. See Hamilton et al. (2016), Holston et al. (2017), Glick (2020), Jorda and Taylor (2019), Del Negro et al. (2019) and Kiley (2020).

the 1951–1955 steady-state interest rate. [20]

Figure 5 Decomposition of the drivers of Global R^*

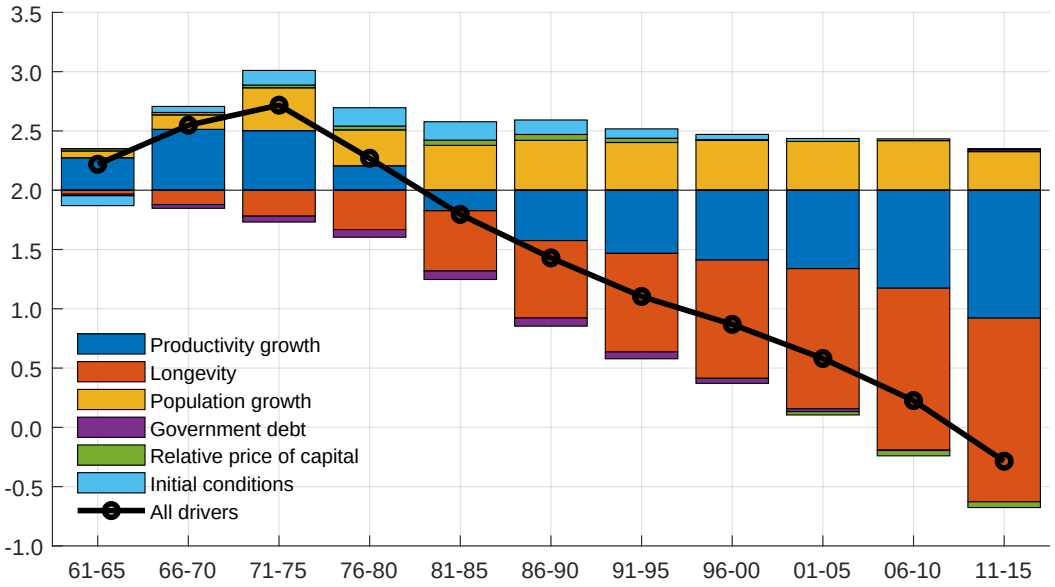

NOTE. The black line with circles shows the baseline path from the recursive simulations. Each bar shows the contribution of an individual driver, computed by constructing a simulation in which only that driver changes over the sample (with all other drivers held fixed at their initial values). The light blue bars for the Initial conditions account for the hypothetical transition from x_0 to x_1^{ss} as defined in Section 4.1. The decomposition is computed relative to the initial steady-state real interest rate, which is set to 2% as described in Section 4.3.

The estimated decline in Global R^* from its peak has been primarily driven by changes in longevity and productivity growth. Increased longevity, due to rising survival probabilities in particular for over-65s, raised the stocks of wealth that households wish to hold to fund their retirements. Higher desired wealth holdings have in turn reduced Global R^*.[21] Slower trend productivity growth has also reduced Global R^*, since lower expected returns on investment have reduced the demand for capital.

Higher population growth in the early part of our sample (the 'baby boom') pushes up slightly on Global R^*, with the effects particularly noticeable in the 1990s and 2000s. Thereafter the effect wanes but not sufficiently to push down on R^* in our model. In line with other studies

[20] That is, the steady-state real interest rate implied by using the 1951–1955 values of the drivers in equation (2), which is an element of x_1^{ss}, as described in Section 4.1. Figure 5 is plotted from 1961–1965 onward because this is the first period in which changes in the drivers can affect the real interest rate (as the safe real rate in the model is a pre-determined variable). Specifically, the real interest rate in 1951–1955 is fixed at the value used to initialise the model (i.e., it is an element of x_0) and so the level in 1956–1960 reflects the adjustment of the real interest rate towards the steady state implied by the 1951–1955 values of the drivers. Since the figure is plotted relative to the 1951–1955 steady state, the only contribution for 1956–1960 is from 'initial conditions' and is therefore omitted.

[21] See Lisack et al. (2021) for more discussion of this mechanism.

(e.g., Sajedi and Thwaites, 2016), the relative price of capital has only a modest effect on the equilibrium real interest rate. Finally, at a global level, according to the calibration of our model, trend movements in government debt are not sufficient to have a material impact on R^*.

Our finding that demographic factors and productivity growth account for the bulk of the decline in the equilibrium real interest rate are consistent with the results of Eggertsson et al. (2019) for the United States. They estimate a 4 percentage point fall in the equilibrium real interest rate between 1970 and 2015, with longevity and productivity growth accounting for 1.8 and 1.9 percentage points respectively. Our Global R^* estimate falls by 2.8 percentage points over the same period, with similarly sized contributions from longevity (-1.4pp) and productivity growth (-1.6pp).

Further comparison with Eggertsson et al. (2019) reveals some differences in the drivers of Global and US R^* between 1970 and 2015. In particular, we find a small positive contribution from population growth, of around 0.2pp, compared with a substantial negative contribution (-1.8pp) for the United States. Similarly, the positive contribution of government debt to Global R^* (0.05pp) is much smaller than the 2 percentage points found for the United States by Eggertsson et al. (2019).[22]

6 Robustness

In this section, we explore the robustness of the OLG-model simulation of Global R^* in two ways. We first examine the sensitivity of the results to alternative assumptions about key simulation inputs, namely the values of model parameters and the paths of the drivers. We then provide a description of the qualitative implications for Global R^* of other potential drivers that are not included in our simulations.

6.1 Sensitivity to Parameter Values and Drivers

To examine the sensitivity of the OLG-model simulation of Global R^*, we re-compute the simulation under alternative assumptions about the values of key parameters and the paths of

[22] A small part of this difference can be accounted for by the different magnitudes of the changes in government debt. Eggertsson et al. (2019) analyse a near tripling of government debt in the United States (from 42% to 118% of annual GDP) whereas our global data imply that the share of government debt roughly doubled over the same period.

the drivers. We consider alternative values for the elasticity of intertemporal substitution (θ), the production-function elasticity (σ), and the group of cohort-specific parameters governing the life-cycle distribution of labour supply, bequests, taxes and monopolistic profits from producers ($\{\rho_\tau, \mathfrak{b}_\tau, \mathfrak{t}_\tau, \xi_\tau\}_{\tau=1}^{T}$). For the drivers, we consider alternative values for the smoothing parameter in the HP filter used for the relative price of capital, government debt to GDP and productivity growth. For each parameter or driver, we specify a discrete set of two alternative assumptions, which, alongside the baseline assumption, gives a set of three possible values for each. We draw random combinations from the total set of alternative assumptions and re-run the recursive simulations for each draw.[23] Appendix B.4 provides further details of this exercise.

Figure 6 Sensitivity of the effects of drivers on Global R^*

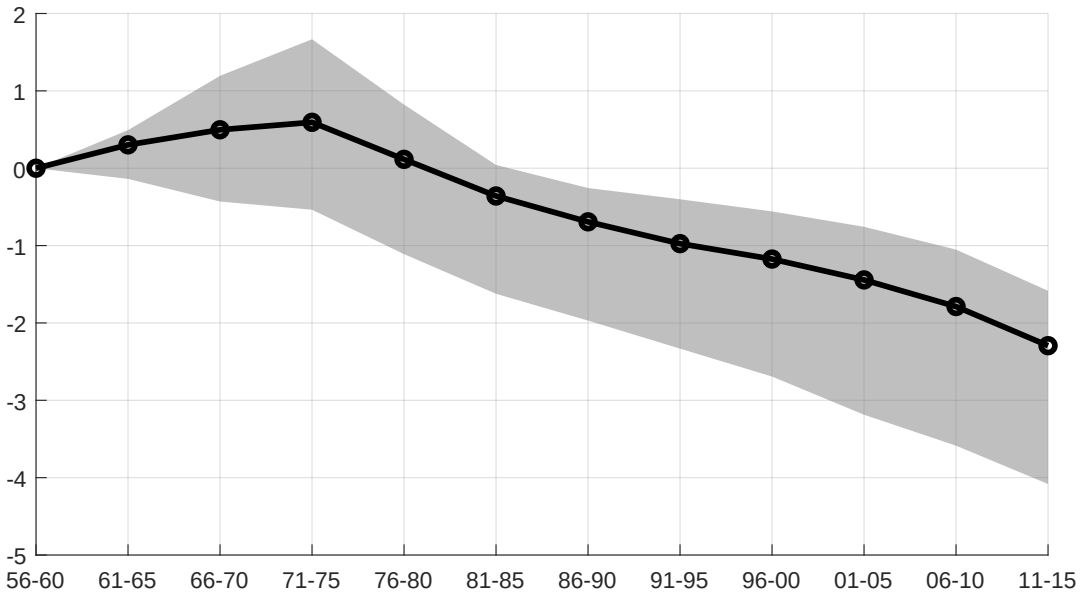

NOTE. The black line with circles shows the effects of the drivers in the baseline simulations, relative to the initial steady state. The grey swathe is the range (minimum to maximum) of simulations from 1,000 random draws of alternative assumptions for model parameters and the paths of the drivers. Appendix B.4 provides full details. The units are annual percentage points.

Figure 6 summarises the results of this experiment. We focus on the effects of the drivers on Global R^*, meaning the sum of the decomposition bars shown in Figure 5, excluding the contribution from initial conditions, computed relative to the 1955 steady state. Examining the results in this form allows us to focus on the effects of the drivers on Global R^*, abstracting from

[23] Although there are only three alternatives for each parameter/driver, we allow a large number of parameters and drivers to vary, which means that the total number of possible combinations is around 40,000. Given the computational overhead of the recursive simulation method, we assess sensitivity using a random sample of 1,000 combinations.

the effects of alternative assumptions on the initial steady state and the transitional dynamics from the initial conditions. It therefore permits a 'like-for-like' assessment of how the effects of the drivers on Global R^* vary under alternative assumptions. The solid black line plots this for our baseline assumptions, and the grey swathe plots the full range – minimum to maximum – of the results obtained drawing from the alternative assumptions.

Figure 6 shows that plausible alternative assumptions generate a wide range of estimates of the effects of the drivers on Global R^*. For the set of alternatives we consider, the range of estimates spans around 2.5 percentage points in 2015, though the range is skewed to the downside of our baseline estimate. Overall, there is a robust finding of a steady decline in Global R^* since the early 1970s.

6.2 Possible Additional Drivers of Global R^*

The structural model brings together five key drivers of Global R^* within a single framework. Nonetheless, there are several potential influences on Global R^* that are not captured by our simulations. Estimating the long-run global trend of each driver for our simulation requires data on a large panel of countries over several decades. So in many cases we cannot include potential drivers within our simulations because the required data is not available. In this section, we outline some of these key missing drivers, drawing on existing research to discuss the likely mechanisms and qualitative effects on Global R^*.

Competition. There is a growing literature documenting a secular decline in the competitiveness of production, and a rise in monopolistic rents, particularly in the United States (De Loecker et al., 2020), but also globally (De Loecker and Eeckhout, 2018; Diez et al., 2018).

In our model, this effect could be captured by an increase in the mark-up, μ, over time. In partial equilibrium, such an increase would reduce the demand for capital, thereby putting downward pressure on the equilibrium real interest rate. However, the general-equilibrium effect of this change would depend on how the resulting profits are distributed to households. If they are distributed proportionally to labour income, an increase in profits would raise the desired savings of these households, pushing down on the interest rate. Conversely, if profits are distributed proportionally to wealth and capital income, an increase in profits would effectively "crowd out" desired savings in the capital stock, and hence push up on the equilibrium real

interest rate.[24]

Eggertsson et al. (2019) assume a rise in mark-ups from 14% to 25% between 1970 and 2015, calibrated to match the decline in the labour share in the United States. They assume that profits are distributed proportionally to labour income, and estimate that this 11 percentage point change reduced the equilibrium real interest rate by around 0.5pp, suggesting a potentially large effect of changes in competition. Using data for 134 countries, De Loecker and Eeckhout (2018) estimate a large rise in mark-ups, from around 10% to 60% between 1980 and 2016.[25]

Consistent global data on mark-ups from 1950 is difficult to obtain, making it challenging to formally incorporate this driver in our simulations. While an increase in the mark-up would likely have a large impact on the simulated path of Global R^*, the direction of the effect is ambiguous without further information on how the resulting profits are distributed.

Rising retirement age. As people live longer, they are likely to work until later in life, either endogenously through increased labour supply in old age, or through a rise in statutory retirement ages. For example, in 2021 the OECD reported that normal retirement ages were set to rise in a majority of OECD countries (OECD, 2021, page 13).

These changes could, in principle, be incorporated in our simulations through changes in the life-cycle profile of age-specific labour supply, ρ_τ. Other things equal, a longer working life flattens out the life-cycle profile of labour income, reducing the incentive to accumulate assets in order to smooth consumption. This would push up on the equilibrium real interest rate, effectively offsetting some of the downward pressure from increased longevity.

Again, consistent data on age-specific labour supply over time for our large panel of countries is not readily available. Moreover, even if this data were available, the effect through this channel may not be very large.[26] Using a similar model to ours, Lisack et al. (2021) find that even a five-year increase in the retirement age, coupled with an assumption that households remain highly productive throughout old age, is not sufficient to offset the downward pressure on the

[24] In fact, allowing agents to buy claims to future firm profits would lead to households endogenously using these claims as an additional savings vehicle for retirement, pushing up on R^* even more than a case where profits are exogenously distributed to wealthier households. For further explanation of this point, see Lisack et al. (2017).

[25] Using data for 74 countries over the same time period, Diez et al. (2018) find that increases in mark-ups appear to have been concentrated in advanced economies, with net mark-ups rising from close to 0 in 1980 to around 0.4 in 2016. In contrast, mark-ups in emerging economies are estimated to have been relatively stable.

[26] Secular changes in broader provision of social security and social insurance by governments could have much larger effects on equilibrium real interest rates (Rachel and Summers, 2019).

equilibrium real interest rate from increased longevity.[27] Even under these assumptions, the additional labour income from a longer working life is small in comparison to the substantial increase in the proportion of life spent in retirement.

Risk and risk aversion. Changes to the quantity or price of risk would lead to an increase in the risk premium, which would push down on the risk-free rate, R^*, for a given return to capital. Indeed, there is evidence that an increase in the 'convenience yield', the premium on government bonds capturing their relative safety and liquidity, has played a significant role in the decline in safe rates of return both in the United States (Del Negro et al., 2017) and globally (Del Negro et al., 2019).

Though the model does not include risk, there is a fixed wedge between the risk-free rate and the return to capital, ϕ^d. In a standard asset-pricing model, this wedge would be affected by both the quantity of risk (i.e., the volatility in the productivity of capital) and the price of risk (i.e., the risk aversion of households). Therefore, in principle, changes in the risk premium over time could be incorporated in our simulations via time variation in ϕ^d. While quantifying this effect is challenging, again due to the lack of data availability for our large panel of countries, it is likely that any secular rise in ϕ^d would reduce Global R^* further.[28]

Health and social insurance. Rachel and Summers (2019) argue that the widespread growth in the provision of publicly-financed social security and healthcare would both reduce the incentives for households to accumulate wealth and crowd out private capital, resulting in upward pressure on Global R^*. By combining the results from two structural models, they estimate that this trend may have increased Global R^* by 2–3pp between 1970 and 2015.[29]

Inequality. There is a large literature documenting a rise in inequality over recent decades, focused on the United States but also in other countries (Alvaredo et al., 2017).

A rise in inequality could potentially affect the equilibrium real interest rate through two

[27] This is a large increase in retirement age compared to current expectations: "Based on legislated measures, the normal retirement age will increase in the OECD on average by about two years in the next four decades, during which life expectancy in old age is projected to increase by about four years." (OECD, 2021, page 12)

[28] Using US data, Caballero et al. (2017) find evidence of increasing risk premia from the 1980s. Not all estimates of risk premia, however, would suggest secular changes in ϕ^d. For example, Gourinchas et al. (2022) estimate the drivers of the consumption to wealth ratio for several advanced economies from 1870. Their estimates suggest a minor role for the risk premium (much smaller than the safe rate), with no strong trend over time.

[29] When accounting for all factors, including some of those considered in the current paper, Rachel and Summers (2019) estimate that Global R^* fell by around 3pp over this period.

channels. First, if increased inequality is caused by an increase in the dispersion of income, this implies higher individual income risk, inducing higher precautionary savings, thereby reducing the real interest rate (Auclert and Rognlie, 2018). Auclert and Rognlie (2017) find that a doubling of the share of labour income earned by the top 1%, in the United States since the 1980s, can account for between 0.45 and 0.85 percentage points decline in the real interest rate. A second channel operates through changes in the composition of the population towards high-income households, who have the highest savings rates. Mian et al. (2021) show that this channel has significantly increased aggregate savings in the United States in recent decades, consistent with the decline in R^*.[30]

While our model incorporates heterogeneity across age groups, there is no within-cohort heterogeneity. Cross-country and long-run data on household-level income and savings is not readily available, making it very difficult to incorporate either channel. However, both channels suggest that a rise in inequality is likely to exert downward pressure on the equilibrium real interest rate.

7 Conclusion

This paper has explored the behaviour and determinants of the global trend equilibrium real interest rate – Global R^* – from 1950 to 2015. Compared with previous studies, we have incorporated both the global nature of the observed fall in real interest rates and a range of potential structural trends that could account for it. To do so, we compiled a rich data set for 31 countries to calibrate and simulate an overlapping-generations model of the world economy, using a recursive method to capture slow-moving beliefs about long-term trends.

Simulations of the model imply that Global R^* increased from the mid-1950s to the mid-1970s before steadily declining to around -0.25% in 2011–2015. This decline is predominantly driven by falling productivity growth and increased longevity.

While monetary policymakers typically focus on cyclical movements in the economy, over the relatively short horizon during which monetary policy can influence demand and inflation, longer-run structural changes can affect the contours of the broader landscape in which monetary policy operates (Bailey, 2022; Bailey et al., 2022). By identifying the key drivers of recent low

[30] Moll et al. (2021) propose an alternative mechanism where inequality results from an increase in automation, which also leads to an increased wedge between the return to capital and the safe interest rate.

levels of Global R^*, our findings can inform judgements about the future policy landscape. For example, without a significant reversal in the long-run trends in productivity growth and population ageing, Global R^* is likely to remain persistently low.

Persistently low Global R^* has many potential implications for the design and implementation of macroeconomic policy frameworks. Some of these implications create additional challenges, such as increasing the probability of reaching the effective lower bound on monetary policy rates, or encouraging a reach-for-yield that may increase risks to financial stability (Powell, 2017). Some may create opportunities, for example by reducing sovereign debt financing costs (Blanchard, 2019). By amplifying spillover effects, the global nature of the decline in equilibrium real rates may heighten the importance of international coordination in the design and implementation of macroeconomic policy frameworks (Fornaro and Romei, 2019).

These challenges and opportunities are important avenues for future research.

References

Adjemian, S., H. Bastani, M. Juillard, F. Mihoubi, G. Perendia, M. Ratto, and S. Villemot (2011): "Dynare: Reference manual, version 4," .

Alvaredo, F., L. Chancel, T. Piketty, E. Saez, and G. Zucman (2017): "Global Inequality Dynamics: New Findings from WID.world," *American Economic Review*, 107, 404–409.

Auclert, A., H. Malmberg, F. Martenet, and M. Rognlie (2021): "Demographics, Wealth, and Global Imbalances in the Twenty-First Century," Working Paper 29161, National Bureau of Economic Research.

Auclert, A. and M. Rognlie (2017): "Aggregate Demand and the Top 1 Percent," *American Economic Review Papers & Proceedings*, 107, 588–92.

——— (2018): "Inequality and Aggregate Demand," Working Paper 24280, National Bureau of Economic Research.

Bailey, A. (2022): "The Economic Landscape: Structural Change, Global R^*, and the Missing Investment Puzzle," *Speech at the Official Monetary and Financial Institutions Forum, 12 July.*

Bailey, A., A. Cesa-Bianchi, M. Garofalo, R. Harrison, N. McLaren, S. Piton, and R. Sajedi (2022): "Structural Change, Global R^*, and the Missing Investment Puzzle," *Supporting paper for Bailey (2022).*

Blanchard, O. (2019): "Public Debt and Low Interest Rates," *American Economic Review*, 109, 1197–1229.

Booth, H. (2006): "Demographic forecasting: 1980 to 2005 in review," *International Journal of Forecasting*, 22, 547–581.

Caballero, R. J., E. Farhi, and P.-O. Gourinchas (2017): "Rents, Technical Change, and Risk Premia Accounting for Secular Trends in Interest Rates, Returns on Capital, Earning Yields, and Factor Shares," *American Economic Review*, 107, 614–20.

De Loecker, J. and J. Eeckhout (2018): "Global Market Power," Working Paper 24768, National Bureau of Economic Research.

De Loecker, J., J. Eeckhout, and G. Unger (2020): "The Rise of Market Power and the Macroeconomic Implications," *The Quarterly Journal of Economics*, 135, 561–644.

Del Negro, M., D. Giannone, M. P. Giannoni, and A. Tambalotti (2017): "Safety, Liquidity, and the Natural Rate of Interest," *Brookings Papers on Economic Activity*, 48, 235–316.

——— (2019): "Global trends in interest rates," *Journal of International Economics*, 118, 248–262.

Diez, F. J., D. Leigh, and S. Tambunlertchai (2018): "Global Market Power and its Macroeconomic Implications," IMF Working Papers 2018/137, International Monetary Fund.

Dowd, K., D. Blake, and A. J. Cairns (2010): "Facing up to uncertain life expectancy: The longevity fan charts," *Demography*, 47, 67–78.

Edge, R. M., T. Laubach, and J. C. Williams (2007): "Learning and shifts in long-run productivity growth," *Journal of Monetary Economics*, 54, 2421–2438.

Eggertsson, G. B., N. R. Mehrotra, and J. A. Robbins (2019): "A model of secular stagnation: Theory and quantitative evaluation," *American Economic Journal: Macroeconomics*, 11, 1–48.

Fornaro, L. and F. Romei (2019): "The Paradox of Global Thrift," *American Economic Review*, 109, 3745–3779.

Giannone, D., M. Lenza, and G. E. Primiceri (2015): "Prior Selection for Vector Autoregressions," *The Review of Economics and Statistics*, 97, 436–451.

Glick, R. (2020): "r* and the global economy," *Journal of International Money and Finance*, 102.

Gourinchas, P.-O., H. Rey, and M. Sauzet (2022): "Global Real Rates: A Secular Approach," CEPR Discussion Papers 16941, C.E.P.R. Discussion Papers.

Hamilton, J. D., E. S. Harris, J. Hatzius, and K. D. West (2016): "The Equilibrium Real Funds Rate: Past, Present, and Future," *IMF Economic Review*, 64, 660–707.

Holston, K., T. Laubach, and J. C. Williams (2017): "Measuring the natural rate of interest: International trends and determinants," *Journal of International Economics*, 108, 59–75.

Jorda, O., M. Schularick, and A. M. Taylor (2017): "Macrofinancial History and the New Business Cycle Facts," *NBER Macroeconomics Annual*, 31, 213–263.

Jorda, O. and A. M. Taylor (2019): "Riders on the Storm," NBER Working Papers 26262, National Bureau of Economic Research.

Kiley, M. T. (2020): "The Global Equilibrium Real Interest Rate: Concepts, Estimates, and Challenges," *Annual Review of Financial Economics*, 12, 305–326.

Laubach, T. and J. C. Williams (2003): "Measuring the Natural Rate of Interest," *The Review of Economics and Statistics*, 85, 1063–1070.

Lisack, N., R. Sajedi, and G. Thwaites (2017): "Demographic trends and the real interest rate," *Bank of England Staff Working Paper No. 701.*

——— (2021): "Population Ageing and the Macroeconomy," *International Journal of Central Banking*, 17, 43–80.

Mian, A., L. Straub, and A. Sufi (2021): "What explains the decline in r*? Rising income inequality versus demographic shifts," *Proceedings of the 2021 Jackson Hole Symposium.*

Moll, B., L. Rachel, and P. Restrepo (2021): "Uneven growth: automation's impact on income and wealth inequality," Bank of England working papers 913, Bank of England.

Moreno Badia, M. M., S. Mbaye, and K. Chae (2018): "Global Debt Database: Methodology and Sources," IMF Working Papers 2018/111, International Monetary Fund.

OECD (2021): "Pensions at a glance," *OECD and G20 Indicators.*

Pesaran, M. H. (2006): "Estimation and Inference in Large Heterogeneous Panels with a Multifactor Error Structure," *Econometrica*, 74, 967–1012.

Powell, J. H. (2017): "Low Interest Rates and the Financial System: A speech at the 77th Annual Meeting of the American Finance Association, Chicago, Illinois, January 7, 2017," Speech 931, Board of Governors of the Federal Reserve System (U.S.).

Rachel, L. and T. D. Smith (2017): "Are Low Real Interest Rates Here to Stay?" *International Journal of Central Banking*, 13, 1–42.

Rachel, L. and L. H. Summers (2019): "On falling neutral real rates, fiscal policy and the risk of secular stagnation," in *Brookings Papers on Economic Activity*, vol. 7.

Sajedi, R. and G. Thwaites (2016): "Why are Real Interest Rates So Low? The Role of the Relative Price of Investment Goods," *IMF Economic Review*, 64, 635–659.

Ziesemer, T. (2021): "Labour-augmenting technical change data for alternative elasticities of substitution: growth, slowdown, and distribution dynamics," *Economics of Innovation and New Technology*, 1–27.

Appendix

A Theoretical Framework: Derivations

The timing convention is such that a subscript t means the variable is determined (known) in period t, and for assets this means the end-of-period quantity. For simplicity, we leave as implicit the expectations operator for future variables.

A.1 Households

A household born in period t lives for maximum T periods, with $\Pi_{t,\tau}$ denoting the unconditional survival probability at age τ, in other words the fraction of the generation born in period t that will survive until age τ. Note that $\Pi_{t,1} = 1$ and $\Pi_{t,T+1} = 0$.

Households are born with no assets. They have access to an asset, a, which pays a net real interest rate r. At each age, they supply ρ_τ units of labour inelastically, for wages $w_{t+\tau-1}$.[31] They also have a stream of non-labour income, $\varpi_{t,\tau}$, which they take as exogenous.

Households maximise their expected lifetime utility, given by:

$$U_t = \sum_{\tau=1}^{T} \beta_\tau \Pi_{t,\tau} \frac{c_{t,\tau}^{1-\theta}}{1-\theta}$$

subject to a budget constraint in each period:

$$c_{t,\tau} = \rho_\tau w_{t+\tau-1} + (1 + r_{t+\tau-2}) a_{t,\tau-1} - a_{t,\tau} + \varpi_{t,\tau}$$

with $a_{t,0} = a_{t,T} = 0$.

Their choice variables are $\{c_{t,\tau}\}_{\tau=1...T}$ and $\{a_{t,\tau}\}_{\tau=1...T-1}$, and we denote by $\lambda_{t,\tau}$ the lagrange multipliers on each budget constraint.

The first order conditions are:

$$\beta_\tau \Pi_{t,\tau} c_{t,\tau}^{-\theta} = \lambda_{t,\tau} \qquad \text{for } \tau = 1...T$$

$$\lambda_{t,\tau} = \lambda_{t,\tau+1}(1 + r_{t+\tau-1}) \qquad \text{for } \tau = 1...T-1$$

Plugging in the first order conditions for consumption into the first order condition for bonds, delivers the familiar Euler equations:

$$\beta_\tau \Pi_{t,\tau} c_{t,\tau}^{-\theta} = \beta_{\tau+1} \Pi_{t,\tau+1} c_{t,\tau+1}^{-\theta} (1 + r_{t+\tau-1}) \qquad \text{for } \tau = 1...T-1$$

or

$$1 = \frac{\beta_{\tau+1}}{\beta_\tau} \frac{\Pi_{t,\tau+1}}{\Pi_{t,\tau}} \left(\frac{c_{t,\tau+1}}{c_{t,\tau}} \right)^{-\theta} (1 + r_{t+\tau-1}) \qquad \text{for } \tau = 1...T-1$$

Thus the household's problem is defined in terms of the $(2T-1)$ choice variables $\{c_{t,\tau}\}_{\tau=1...T}$ and $\{a_{t,\tau}\}_{\tau=1...T-1}$, the $(T-1)$ Euler equations, and the T budget constraints.

[31] $t + \tau - 1$ is the period in which the generation born in period t is aged τ.

A.1.1 Recursive form

So far, it has been useful to consider the maximisation problem of the generation born in period t, over the T periods of their life. To write the problem recursively, however, we now express these equations for the T generations alive in a given period t.

First redefine each variable $x_{t,\tau}$, to be the variable x for the household aged τ in period t. We can write the budget constraint of household aged $\tau = 1...T$ in period t as:

$$c_{t,\tau} = \rho_{t,\tau} w_t + (1 + r_{t-1}) a_{t-1,\tau-1} - a_{t,\tau} + \varpi_{t,\tau} \quad \text{for } \tau = 1...T \tag{A.1}$$

The Euler equation for household aged $\tau = 1...T-1$ in period t is:

$$1 = \frac{\beta_{\tau+1}}{\beta_\tau} \frac{\Pi_{t+1,\tau+1}}{\Pi_{t,\tau}} \left(\frac{c_{t+1,\tau+1}}{c_{t,\tau}} \right)^{-\theta} (1 + r_t) \quad \text{for } \tau = 1...T-1 \tag{A.2}$$

with $\Pi_{t,1} = 1$ and $\Pi_{t,T+1} = 0$ for all t.

A.2 Firms and Financial Intermediary

The problem of the firms and financial intermediary was described in full detail in Section 2.

A.3 Government

The government has a stock of debt, G on which it pays interest, r. This interest payment is financed by lump sum taxes levied on households $\mathcal{T}_t$. Hence their budget constraint is given by

$$G_t = (1 + r_{t-1}) G_{t-1} - \mathcal{T}_t$$

This can be written in ratio to output:

$$\frac{G_t}{Y_t} = (1 + r_{t-1}) \frac{G_{t-1}}{Y_t} - \frac{\mathcal{T}_t}{Y_t} \tag{A.3}$$

A.4 Aggregation and Market Clearing

Population Growth. Let N_t be the size of the cohort born at time t. Let $n_t \equiv \frac{N_t - N_{t-1}}{N_{t-1}}$ be the net growth rate of consecutive cohorts.

Total labour supply is given by:

$$L_t = \sum_{\tau=1}^{T} \rho_{t,\tau} \Pi_{t,\tau} N_{t-\tau+1} \tag{A.4}$$

Asset markets. The aggregate assets of the household are either used to buy the stock of government bonds, or turned into capital by the financial intermediary

$$p_t^k K_t + G_t = \sum_{\tau=1}^{T} N_{t-\tau+1} \Pi_{t,\tau} a_{t,\tau} \tag{A.5}$$

Households that die between periods leave their assets, along with the return, as accidental bequests. We can define aggregate accidental bequests as

$$\mathcal{B}_t = (1+r_{t-1})\sum_{\tau=1}^{T}(1-\frac{\Pi_{t,\tau+1}}{\Pi_{t-1,\tau}})\Pi_{t-1,\tau}N_{t-\tau}a_{t-1,\tau} \tag{A.6}$$

Goods markets. Define aggregate consumption:

$$C_t = \sum_{\tau=1}^{T} N_{t-\tau+1}\Pi_{t,\tau}c_{t,\tau} \tag{A.7}$$

We can sum up the budget constraints of all the households alive in a given period:

$$\begin{aligned} C_t &= w_t\sum_{\tau=1}^{T} N_{t-\tau+1}\Pi_{t,\tau}\rho_{t,\tau} - \sum_{\tau=1}^{T} N_{t-\tau+1}\Pi_{t,\tau}a_{t,\tau} + (1+r_{t-1})\sum_{\tau=1}^{T} N_{t-\tau+1}\Pi_{t,\tau}a_{t-1,\tau-1} \\ &\quad + \sum_{\tau=1}^{T} N_{t-\tau+1}\Pi_{t,\tau}\varpi_{t,\tau} \\ &= L_t w_t - p_t^k K_t - G_t + (1+r_{t-1})\sum_{\tau=1}^{T} N_{t-\tau+1}\Pi_{t,\tau}a_{t-1,\tau-1} + \sum_{\tau=1}^{T} N_{t-\tau+1}\Pi_{t,\tau}\varpi_{t,\tau} \end{aligned}$$

The non-labour income of the household, ϖ, comprises of the monopolistic profit of the retailer, the rebate on the capital spread friction, the accidental bequests, minus the lump sum taxes paid to the government. Since we have defined these objects as aggregates in each period, we need to distribute them among the different generations.

$$\Pi_{t,\tau}N_{t-\tau+1}\varpi_{t,\tau} = \xi_\tau\Xi_t + \varphi_\tau\varphi\Phi_t^d + \mathfrak{b}_\tau\mathcal{B}_t - \mathfrak{t}_\tau\mathcal{T}_t \tag{A.8}$$

with $\sum_{\tau=1}^{T}\xi_\tau = \sum_{\tau=1}^{T}\varphi_\tau = \sum_{\tau=1}^{T}\mathfrak{b}_\tau = \sum_{\tau=1}^{T}\mathfrak{t}_{t,\tau} = 1$. Plugging this into the aggregate budget constraint above we have

$$C_t = L_t w_t - p_t^k K_t - G_t + (1+r_{t-1})\sum_{\tau=1}^{T} N_{t-\tau+1}\Pi_{t,\tau}a_{t-1,\tau-1} + \Xi_t + \varphi\Phi_t^d + \mathcal{B}_t - \mathcal{T}_t$$

Bringing in the government budget constraint, we have

$$\begin{aligned} C_t &= L_t w_t - p_t^k K_t - G_t + (1+r_{t-1})\sum_{\tau=1}^{T} N_{t-\tau+1}\Pi_{t,\tau}a_{t-1,\tau-1} + \Xi_t + \varphi\Phi_t^d + \mathcal{B}_t + G_t - (1+r_{t-1})G_{t-1} \\ &= L_t w_t - p_t^k K_t + (1+r_{t-1})\sum_{\tau=1}^{T} N_{t-\tau+1}\Pi_{t,\tau}a_{t-1,\tau-1} + \Xi_t + \varphi\Phi_t^d + \mathcal{B}_t - (1+r_{t-1})G_{t-1} \end{aligned}$$

Bringing in the definition of aggregate bequests, we have

$$\begin{aligned}
C_t &= L_t w_t - p_t^k K_t + (1+r_{t-1})\sum_{\tau=1}^{T} N_{t-\tau+1}\Pi_{t,\tau}a_{t-1,\tau-1} + \Xi_t + \varphi\Phi_t^d \\
&\quad +(1+r_{t-1})\sum_{\tau=1}^{T}(1-\frac{\Pi_{t,\tau+1}}{\Pi_{t-1,\tau}})\Pi_{t-1,\tau}N_{t-\tau}a_{t-1,\tau} - (1+r_{t-1})G_{t-1} \\
&= L_t w_t - p_t^k K_t + (1+r_{t-1})\sum_{\tau=1}^{T} N_{t-\tau+1}\Pi_{t,\tau}a_{t-1,\tau-1} + (1+r_{t-1})\sum_{\tau=1}^{T}(1-\frac{\Pi_{t,\tau+1}}{\Pi_{t-1,\tau}})\Pi_{t-1,\tau}N_{t-\tau}a_{t-1,\tau} \\
&\quad +\Xi_t + \varphi\Phi_t^d - (1+r_{t-1})G_{t-1} \\
&= L_t w_t - p_t^k K_t + (1+r_{t-1})\sum_{\tau=0}^{T-1} N_{t-\tau}\Pi_{t,\tau+1}a_{t-1,\tau} + (1+r_{t-1})\sum_{\tau=1}^{T}(1-\frac{\Pi_{t,\tau+1}}{\Pi_{t-1,\tau}})\Pi_{t-1,\tau}N_{t-\tau}a_{t-1,\tau} \\
&\quad +\Xi_t + \varphi\Phi_t^d - (1+r_{t-1})G_{t-1} \\
&= L_t w_t - p_t^k K_t + (1+r_{t-1})\sum_{\tau=1}^{T} N_{t-\tau}\Pi_{t,\tau+1}a_{t-1,\tau} + (1+r_{t-1})\sum_{\tau=1}^{T}(1-\frac{\Pi_{t,\tau+1}}{\Pi_{t-1,\tau}})\Pi_{t-1,\tau}N_{t-\tau}a_{t-1,\tau} \\
&\quad +\Xi_t + \varphi\Phi_t^d - (1+r_{t-1})G_{t-1}
\end{aligned}$$

Where the final line follows from the fact that $\Pi_{t,T+1} = 0$, and $a_{t,0} = 0$. Bringing terms together, we have

$$\begin{aligned}
C_t &= L_t w_t - p_t^k K_t + (1+r_{t-1})\sum_{\tau=1}^{T}\left\{\Pi_{t,\tau+1} + (1-\frac{\Pi_{t,\tau+1}}{\Pi_{t-1,\tau}})\Pi_{t-1,\tau}\right\}N_{t-\tau}a_{t-1,\tau} + \Xi_t \\
&\quad +\varphi\Phi_t^d - (1+r_{t-1})G_{t-1} \\
&= L_t w_t - p_t^k K_t + (1+r_{t-1})\sum_{\tau=1}^{T}\Pi_{t-1,\tau}N_{t-\tau}a_{t-1,\tau} + \Xi_t + \varphi\Phi_t^d - (1+r_{t-1})G_{t-1} \\
&= L_t w_t - p_t^k K_t + (1+r_{t-1})\sum_{\tau=1}^{T}\Pi_{t-1,\tau}N_{(t-1)-\tau+1}a_{t-1,\tau} + \Xi_t + \varphi\Phi_t^d - (1+r_{t-1})G_{t-1}
\end{aligned}$$

Bringing in the period $(t-1)$ asset market clearing condition, we have

$$\begin{aligned}
C_t &= L_t w_t - p_t^k K_t + (1+r_{t-1})\left(p_{t-1}^k K_{t-1} + G_{t-1}\right) + \Xi_t + \varphi\Phi_t^d - (1+r_{t-1})G_{t-1} \\
&= L_t w_t - p_t^k K_t + (1+r_{t-1})\left(p_{t-1}^k K_{t-1}\right) + \Xi_t + \varphi\Phi_t^d \\
&= L_t w_t + (1+r_{t-1})p_{t-1}^k K_{t-1} - p_t^k K_t + \Xi_t + \varphi\Phi_t^d
\end{aligned}$$

Consider first the term on capital

$$\begin{aligned}
(1+r_{t-1})p_{t-1}^k K_{t-1} - p_t^k K_t &= \left((1+r_t^k-\delta)\frac{p_t^k}{p_{t-1}^k} - \phi^d\right)p_{t-1}^k K_{t-1} - p_t^k K_t \\
&= (1+r_t^k-\delta)p_t^k K_{t-1} - \phi^d p_{t-1}^k K_{t-1} - p_t^k K_t \\
&= r_t^k p_t^k K_{t-1} - p_t^k(K_t - (1-\delta)K_{t-1}) - \phi^d p_{t-1}^k K_{t-1} \\
&= r_t^k p_t^k K_{t-1} - p_t^k I_t - \Phi_t^d
\end{aligned}$$

where we have defined investment as $I_t = K_t - (1-\delta)K_{t-1}$. Plugging this back in to the above

$$C_t = L_t w_t + r_t^k p_t^k K_{t-1} - p_t^k I_t - \Phi_t^d + \Xi_t + \varphi \Phi_t^d$$

$$C_t + p_t^k I_t = L_t w_t + r_t^k p_t^k K_{t-1} + \Xi_t - (1-\varphi)\Phi_t^d$$

The zero-profit condition of the intermediate goods producer implies

$$L_t w_t + r_t^k p_t^k K_{t-1} = \frac{1}{1+\mu_t} Y_t$$

and using the definition of the profit of the retailer, we can write the right hand side of the above as

$$L_t w_t + r_t^k p_t^k K_{t-1} + \Xi_t = \frac{1}{1+\mu_t} Y_t + \frac{\mu_t}{1+\mu_t} Y_t = Y_t$$

Plugging this in, we have the aggregate resource constraint

$$Y_t = C_t + p_t^k I_t + (1-\varphi)\Phi_t^d$$

This says that all goods produced must either be consumed or invested or paid towards the resource cost associated with the risk premium.

A.5 Exogenous Processes

The remaining exogenous processes (the 'drivers') in the model are described by random walks, to facilitate the recursive simulation method.

$$n_t = n_{t-1} + \epsilon_t^n \tag{A.9}$$

$$\Pi_{t,\tau} = \Pi_{t-1,\tau} + \epsilon_t^{\Pi_\tau} \qquad \text{for } \tau = 2, ...T \tag{A.10}$$

$$e_t = e_{t-1} + \epsilon_t^e \tag{A.11}$$

$$\frac{G_t}{Y_t} = \frac{G_{t-1}}{Y_{t-1}} + \epsilon_t^G \tag{A.12}$$

$$p_t^k = p_{t-1}^k + \epsilon_t^{pk} \tag{A.13}$$

$$\tag{A.14}$$

A.6 Stationarising the Model

The model has two sources of growth in steady state: technological growth at rate e_t and population growth at rate n_t.

The size of the working population at date t is:

$$L_t \equiv \sum_{\tau=1}^{T} \rho_{\tau,t} N_{t,\tau}$$

and our objective is to express the growth rate of the working population in terms of the underlying growth drivers in the model.

The size of each cohort, as a share of the total effective labour supply is given by:

$$n_{t,\tau} \equiv \frac{N_{t,\tau}}{L_t}$$

which can be defined recursively for $\tau = 2, \ldots, T$, by noting that

$$n_{t,\tau} = \frac{N_{t,\tau}}{L_t} = \frac{\frac{\Pi_{t-\tau+1,\tau}}{\Pi_{t-\tau+1,\tau-1}} N_{t-1,\tau-1}}{L_{t-1}} \frac{L_{t-1}}{L_t}$$

so that

$$n_{t,\tau} = \frac{\Pi_{t-\tau+1,\tau}}{\Pi_{t-\tau+1,\tau-1}} n_{t-1,\tau-1} \left(1 + l_t\right)^{-1} \qquad \tau = 2, \ldots, T \tag{A.15}$$

where l is the net growth rate of the working population.

For $n_{t,1}$, we have:

$$n_{t,1} = \frac{N_{t,1}}{L_t} = \frac{\left(1 + n_t\right) N_{t-1,1}}{L_{t-1}} \frac{L_{t-1}}{L_t}$$

so that

$$n_{t,1} = n_{t-1,1} \frac{1 + n_t}{1 + l_t} \tag{A.16}$$

The preceding equations show how we can determine the population shares in terms of recursive equations which depend on ex-post survival probabilities and total labour force growth.

Growth of the working population satisfies:

$$1 + l_t = \frac{L_t}{L_{t-1}} = \frac{\sum_{\tau=1}^{T} \rho_{t,\tau} N_{t,\tau}}{L_{t-1}}$$

which we can write as

$$1 + l_t = \sum_{\tau=1}^{T} \rho_{t,\tau} m_{t,\tau} \tag{A.17}$$

where

$$m_{t,\tau} \equiv \frac{N_{t,\tau}}{L_{t-1}}$$

is defined as the size of each cohort relative to the size of the *previous period's* working population.[32]

Following the same steps as for $n_{t,\tau}$, $m_{t,\tau}$ can be expressed recursively by noting that:

$$m_{t,\tau} = \frac{\frac{\Pi_{t-\tau+1,\tau}}{\Pi_{t-\tau+1,\tau-1}} N_{t-1,\tau-1}}{L_{t-2}} \frac{L_{t-2}}{L_{t-1}}$$

so that

$$m_{t,\tau} = \frac{\Pi_{t-\tau+1,\tau}}{\Pi_{t-\tau+1,\tau-1}} m_{t-1,\tau-1} \left(1 + l_{t-1}\right)^{-1} \qquad \tau = 2, \ldots, T \tag{A.18}$$

and

$$m_{t,1} = \frac{1 + n_t}{1 + l_{t-1}} m_{t-1,1} \tag{A.19}$$

[32] To compute the steady-state values of m note that:

$$m_{t,\tau} = \frac{N_{t,\tau}}{L_t} \frac{L_t}{L_{t-1}} = n_{t,\tau} \left(1 + l_t\right)$$

so in steady state, we have

$$m_\tau = \left(1 + l\right) n_\tau \qquad \tau = 1, \ldots, T$$

Write the production function in per effective units of labour terms

$$\frac{Y_t}{E_t L_t} = \left(\alpha \left(\frac{K_{t-1}}{E_t L_t} \right)^{\frac{\sigma-1}{\sigma}} + (1-\alpha) \right)^{\frac{\sigma}{\sigma-1}}$$

Redefine lower case variables as per effective units of labour, $z_t = Z_t / E_t L_t$, so that

$$\begin{aligned} k_{t-1} &= \frac{K_{t-1}}{E_{t-1} L_{t-1}} \\ &= \frac{K_{t-1}}{E_t L_t} \frac{E_t L_t}{E_{t-1} L_{t-1}} \\ &= \frac{K_{t-1}}{E_t L_t} \frac{E_t}{E_{t-1}} \frac{L_t}{L_{t-1}} \\ &= \frac{K_{t-1}}{E_t L_t} (1+e_t)(1+l_t) \end{aligned}$$

This means we can write

$$y_t = \left(\alpha \left(\frac{k_{t-1}}{(1+e_t)(1+l_t)} \right)^{\frac{\sigma-1}{\sigma}} + (1-\alpha) \right)^{\frac{\sigma}{\sigma-1}} \tag{A.20}$$

$$\widetilde{\Xi}_t = \frac{\mu_t}{(1+\mu_t)} y_t \tag{A.21}$$

The factor prices can be written

$$r_t^k = \frac{1}{(1+\mu_t)} \alpha \frac{1}{p_t^k} \left(\frac{(1+e_t)(1+l_t) y_t}{k_{t-1}} \right)^{\frac{1}{\sigma}} \tag{A.22}$$

$$\widetilde{w}_t = \frac{1}{(1+\mu_t)} (1-\alpha) \left(y_t \right)^{\frac{1}{\sigma}} \tag{A.23}$$

Where we define $\widetilde{w}_t \equiv w_t / E_t$.

We can redefine the costs from the capital spread:

$$\widetilde{\Phi}_t^d = \phi^d p_{t-1}^k k_{t-1} / (1+e_t)(1+l_t) \tag{A.24}$$

and the aggregate bequests

$$\begin{aligned} \widetilde{\mathcal{B}}_t &= (1+r_{t-1}) \sum_{\tau=1}^{T} (1 - \frac{\Pi_{t,\tau+1}}{\Pi_{t-1,\tau}}) \frac{\Pi_{t-1,\tau} N_{t-\tau}}{E_t L_t} a_{t-1,\tau} \\ &= (1+r_{t-1}) \sum_{\tau=1}^{T} (1 - \frac{\Pi_{t,\tau+1}}{\Pi_{t-1,\tau}}) \frac{\Pi_{t-1,\tau} N_{t-\tau}}{L_{t-1}} \frac{a_{t-1,\tau}}{E_{t-1}} \frac{E_{t-1} L_{t-1}}{E_t L_t} \\ &= (1+r_{t-1}) \sum_{\tau=1}^{T} (1 - \frac{\Pi_{t,\tau+1}}{\Pi_{t-1,\tau}}) n_{t-1,\tau} \tilde{a}_{t-1,\tau} \frac{E_{t-1} L_{t-1}}{E_t L_t} \\ &= \frac{(1+r_{t-1})}{(1+e_t)(1+l_t)} \sum_{\tau=1}^{T} (1 - \frac{\Pi_{t,\tau+1}}{\Pi_{t-1,\tau}}) n_{t-1,\tau} \tilde{a}_{t-1,\tau} \end{aligned} \tag{A.25}$$

We can also rewrite the period t Euler equations

$$\begin{aligned}
1 &= \frac{\beta_{\tau+1}}{\beta_\tau}\frac{\Pi_{t+1,\tau+1}}{\Pi_{t,\tau}}\left(\frac{c_{t+1,\tau+1}}{c_{t,\tau}}\right)^{-\theta}(1+r_t) \\
&= \frac{\beta_{\tau+1}}{\beta_\tau}\frac{\Pi_{t+1,\tau+1}}{\Pi_{t,\tau}}\left(\frac{c_{t+1,\tau+1}}{E_{t+1}}\frac{E_t}{c_{t,\tau}}\frac{E_{t+1}}{E_t}\right)^{-\theta}(1+r_t) \\
&= \frac{\beta_{\tau+1}}{\beta_\tau}\frac{\Pi_{t+1,\tau+1}}{\Pi_{t,\tau}}\left(\frac{\tilde{c}_{t+1,\tau+1}}{\tilde{c}_{t,\tau}}(1+e_{t+1})\right)^{-\theta}(1+r_t) \\
&= \frac{\beta_{\tau+1}}{\beta_\tau}\frac{\Pi_{t+1,\tau+1}}{\Pi_{t,\tau}}\left(\frac{\tilde{c}_{t+1,\tau+1}}{\tilde{c}_{t,\tau}}\right)^{-\theta}(1+e_{t+1})^{-\theta}(1+r_t) \qquad \text{for } \tau = 1,...T-1 \qquad \text{(A.26)}
\end{aligned}$$

Hence aggregate consumption can be written

$$\begin{aligned}
c_t &= \sum_{\tau=1}^{T}\frac{N_{t-\tau+1}\Pi_{t,\tau}}{L_t}\frac{c_{t,\tau}}{E_t} \\
&= \sum_{\tau=1}^{T} n_{t,\tau}\tilde{c}_{t,\tau} \qquad \text{(A.27)}
\end{aligned}$$

The non-labour income can be written

$$\begin{aligned}
\varpi_{t,\tau} &= \frac{1}{\Pi_{t,\tau}N_{t-\tau+1}}\left(\xi_\tau\Xi_t + \varphi_\tau\varphi\Phi_t^d + \mathfrak{b}_\tau\mathcal{B}_t - \mathfrak{t}_\tau\mathcal{T}_t\right) \\
&= \frac{E_tL_t}{\Pi_{t,\tau}N_{t-\tau+1}}\left(\xi_\tau\widetilde{\Xi}_t + \varphi_\tau\varphi\widetilde{\Phi}_t^d + \mathfrak{b}_\tau\widetilde{\mathcal{B}}_t - \mathfrak{t}_\tau\widetilde{\mathcal{T}}_t\right) \\
&= \frac{E_t}{n_{t,\tau}}\left(\xi_\tau\widetilde{\Xi}_t + \varphi_\tau\varphi\widetilde{\Phi}_t^d + \mathfrak{b}_\tau\widetilde{\mathcal{B}}_t - \mathfrak{t}_\tau\widetilde{\mathcal{T}}_t\right) \\
n_{t,\tau}\widetilde{\varpi}_{t,\tau} &= \xi_\tau\widetilde{\Xi}_t + \varphi_\tau\varphi\widetilde{\Phi}_t^d + \mathfrak{b}_\tau\widetilde{\mathcal{B}}_t - \mathfrak{t}_\tau\widetilde{\mathcal{T}}_t \qquad \text{(A.28)}
\end{aligned}$$

and the budget constraints can be written as

$$\begin{aligned}
\tilde{c}_{t,\tau} &= \rho_{t,\tau}\widetilde{w}_t + (1+r_{t-1})\tilde{a}_{t-1,\tau-1}\frac{E_{t-1}}{E_t} - \tilde{a}_{t,\tau} + \widetilde{\varpi}_{t,\tau} \\
&= \rho_{t,\tau}\widetilde{w}_t + \frac{(1+r_{t-1})}{(1+e_t)}\tilde{a}_{t-1,\tau-1} - \tilde{a}_{t,\tau} + \widetilde{\varpi}_{t,\tau} \qquad \text{for } \tau = 1,...T \qquad \text{(A.29)}
\end{aligned}$$

The capital spread definition remains unchanged

$$(1+r_t) = \frac{1+r_{t+1}^k-\delta}{1+\phi^d}\frac{p_{t+1}^k}{p_t^k} \qquad \text{(A.30)}$$

The asset market clearing condition can be written

$$p_t^k k_t + g_t = \sum_{\tau=1}^{T} n_{t,\tau}\tilde{a}_{t,\tau} \qquad \text{(A.31)}$$

Writing the government budget constraint in ratio to total output:

$$\begin{aligned}\frac{G_t}{Y_t} &= (1+r_{t-1})\frac{G_{t-1}}{Y_{t-1}}\frac{Y_{t-1}}{Y_t} - \frac{\mathcal{T}_t}{Y_t} \\ \frac{g_t}{y_t} &= (1+r_{t-1})\frac{g_{t-1}}{y_{t-1}}\frac{y_{t-1}}{y_t}\frac{E_{t-1}L_{t-1}}{E_tL_t} - \frac{\widetilde{\mathcal{T}}_t}{y_t} \\ &= (1+r_{t-1})\frac{g_{t-1}}{y_{t-1}}\frac{y_{t-1}/y_t}{(1+e_t)(1+l_t)} - \frac{\widetilde{\mathcal{T}}_t}{y_t} \end{aligned} \tag{A.32}$$

The exogenous processes remain unchanged

$$n_t = n_{t-1} + \epsilon_t^n \tag{A.33}$$
$$\Pi_{t,\tau} = \Pi_{t-1,\tau} + \epsilon_t^{\Pi_\tau} \qquad \text{for } \tau = 1,...T \tag{A.34}$$
$$e_t = e_{t-1} + \epsilon_t^e \tag{A.35}$$
$$\frac{g_t}{y_t} = \frac{g_{t-1}}{y_{t-1}} + \epsilon_t^G \tag{A.36}$$
$$p_t^k = p_{t-1}^k + \epsilon_t^{pk} \tag{A.37}$$
$$\tag{A.38}$$

A.7 Final Model Equations

$$n_{t,\tau} = \frac{\Pi_{t-\tau+1,\tau}}{\Pi_{t-\tau+1,\tau-1}} n_{t-1,\tau-1}\,(1+l_t)^{-1} \qquad \tau = 2,\ldots,T \tag{A.39}$$

$$n_{t,1} = n_{t-1,1}\frac{1+n_t}{1+l_t} \tag{A.40}$$

$$1 + l_t = \sum_{\tau=1}^{T} \rho_{t,\tau} m_{t,\tau} \tag{A.41}$$

$$m_{t,\tau} = \frac{\Pi_{t-\tau+1,\tau}}{\Pi_{t-\tau+1,\tau-1}} m_{t-1,\tau-1}\,(1+l_{t-1})^{-1} \qquad \tau = 2,\ldots,T \tag{A.42}$$

$$m_{t,1} = \frac{1+n_t}{1+l_{t-1}} m_{t-1,1} \tag{A.43}$$

$$y_t = \left(\alpha\left(\frac{k_{t-1}}{(1+e_t)(1+l_t)}\right)^{\frac{\sigma-1}{\sigma}} + (1-\alpha)\right)^{\frac{\sigma}{\sigma-1}} \tag{A.44}$$

$$\widetilde{\Xi}_t = \frac{\mu_t}{(1+\mu_t)} y_t \tag{A.45}$$

$$r_t^k = \frac{1}{(1+\mu_t)}\alpha\frac{1}{p_t^k}\left(\frac{(1+e_t)(1+l_t)y_t}{k_{t-1}}\right)^{\frac{1}{\sigma}} \tag{A.46}$$

$$\widetilde{w}_t = \frac{1}{(1+\mu_t)}(1-\alpha)\,(y_t)^{\frac{1}{\sigma}} \tag{A.47}$$

$$1 = \frac{\beta_{\tau+1}}{\beta_\tau}\frac{\Pi_{t+1,\tau+1}}{\Pi_{t,\tau}}\left(\frac{\tilde{c}_{t+1,\tau+1}}{\tilde{c}_{t,\tau}}\right)^{-\theta}(1+e_{t+1})^{-\theta}(1+r_t) \qquad \text{for } \tau = 1,...T-1 \tag{A.48}$$

$$c_t = \sum_{\tau=1}^{T} n_{t,\tau}\tilde{c}_{t,\tau} \tag{A.49}$$

$$\tilde{c}_{t,\tau} = \rho_{t,\tau}\widetilde{w}_t + \frac{(1+r_{t-1})}{(1+e_t)}\tilde{a}_{t-1,\tau-1} - \tilde{a}_{t,\tau} + \widetilde{\varpi}_{t,\tau} \qquad \text{for } \tau = 1,...T \tag{A.50}$$

$$n_{t,\tau}\widetilde{\varpi}_{t,\tau} = \xi_\tau \widetilde{\Xi}_t + \varphi_\tau \varphi \widetilde{\Phi}^d_t + \mathfrak{b}_\tau \widetilde{\mathcal{B}}_t - \mathfrak{t}_\tau \widetilde{\mathcal{T}}_t \qquad \text{for } \tau = 1, ...T \tag{A.51}$$

$$(1 + r_t) = \frac{1 + r^k_{t+1} - \delta}{1 + \phi^d} \frac{p^k_{t+1}}{p^k_t} \tag{A.52}$$

$$p^k_t k_t + g_t = \sum_{\tau=1}^{T} n_{t,\tau} \tilde{a}_{t,\tau} \tag{A.53}$$

$$\frac{g_t}{y_t} = (1 + r_{t-1}) \frac{g_{t-1}}{y_{t-1}} \frac{y_{t-1}/y_t}{(1 + e_t)(1 + l_t)} - \frac{\widetilde{\mathcal{T}}_t}{y_t} \tag{A.54}$$

$$\widetilde{\Phi}^d_t = \phi^d p^k_{t-1} k_{t-1} / (1 + e_t)(1 + l_t) \tag{A.55}$$

$$\widetilde{\mathcal{B}}_t = \frac{(1 + r_{t-1})}{(1 + e_t)(1 + l_t)} \sum_{\tau=1}^{T} (1 - \frac{\Pi_{t,\tau+1}}{\Pi_{t-1,\tau}}) n_{t-1,\tau} \tilde{a}_{t-1,\tau} \tag{A.56}$$

$$n_t = n_{t-1} + \epsilon^n_t \tag{A.57}$$

$$\Pi_{t,\tau} = \Pi_{t-1,\tau} + \epsilon^{\Pi_\tau}_t \qquad \text{for } \tau = 1, ...T \tag{A.58}$$

$$e_t = g_{t-1} + \epsilon^e_t \tag{A.59}$$

$$\frac{g_t}{y_t} = \frac{g_{t-1}}{y_{t-1}} + \epsilon^G_t \tag{A.60}$$

$$p^k_t = p^k_{t-1} + \epsilon^{pk}_t \tag{A.61}$$

A.8 Steady-State Equations

The steady-state version of the model

$$l = n \tag{A.62}$$

$$n_\tau = \frac{\Pi_\tau}{\Pi_{\tau-1}} n_{\tau-1} (1 + l)^{-1} \qquad \tau = 2, \ldots, T \tag{A.63}$$

$$1 + l = \sum_{\tau=1}^{T} \rho_\tau m_\tau \tag{A.64}$$

$$m_\tau = (1 + l) n_\tau \qquad \text{for } \tau = 1, \ldots, T \tag{A.65}$$

$$y = \left(\alpha \left(\frac{k}{(1 + e)(1 + l)} \right)^{\frac{\sigma - 1}{\sigma}} + (1 - \alpha) \right)^{\frac{\sigma}{\sigma - 1}} \tag{A.66}$$

$$\widetilde{\Xi} = \frac{\mu}{(1 + \mu)} y \tag{A.67}$$

$$r^k = \frac{1}{(1 + \mu)} \alpha \frac{1}{p^k} \left(\frac{(1 + e)(1 + l) y}{k} \right)^{\frac{1}{\sigma}} \tag{A.68}$$

$$\widetilde{w} = \frac{1}{(1 + \mu)} (1 - \alpha) (y)^{\frac{1}{\sigma}} \tag{A.69}$$

$$1 = \frac{\beta_{\tau+1}}{\beta_\tau} \frac{\Pi_{\tau+1}}{\Pi_\tau} \left(\frac{\tilde{c}_{\tau+1}}{\tilde{c}_\tau} \right)^{-\theta} (1 + e)^{-\theta} (1 + r) \qquad \text{for } \tau = 1, ...T - 1 \tag{A.70}$$

$$c = \sum_{\tau=1}^{T} n_\tau \tilde{c}_\tau \tag{A.71}$$

$$\tilde{c}_\tau = \rho_\tau \widetilde{w} + \frac{(1 + r)}{(1 + e)} \tilde{a}_{\tau-1} - \tilde{a}_\tau + \widetilde{\varpi}_\tau \qquad \text{for } \tau = 1, ...T \tag{A.72}$$

$$n_\tau \widetilde{\varpi}_\tau = \xi_\tau \widetilde{\Xi} + \varphi_\tau \varphi \widetilde{\Phi}^d + \mathfrak{b}_\tau \widetilde{\mathcal{B}} - \mathfrak{t}_\tau \widetilde{\mathcal{T}} \qquad \text{for } \tau = 1, ...T \tag{A.73}$$

$$(1+r) = \frac{1+r^k-\delta}{1+\phi^d} \tag{A.74}$$

$$p^k k + g = \sum_{\tau=1}^{T} n_\tau \tilde{a}_\tau \tag{A.75}$$

$$\left(\frac{(1+r)}{(1+e)(1+l)} - 1 \right) \frac{g}{y} = \frac{\widetilde{\mathcal{T}}}{y} \tag{A.76}$$

$$\widetilde{\Phi}^d = \phi^d p^k k / (1+e)(1+l) \tag{A.77}$$

$$\widetilde{\mathcal{B}} = \frac{(1+r)}{(1+e)(1+l)} \sum_{\tau=1}^{T} (1 - \frac{\Pi_{\tau+1}}{\Pi_\tau}) n_\tau \tilde{a}_\tau \tag{A.78}$$

B Theoretical Framework: Computational Details

This Appendix provides further details of the recursive simulation approach, the calibration of parameters, the process for setting the initial conditions of the simulation and the exercise to examine sensitivity of the results to alternative assumptions.

B.1 Recursive simulation method

As noted in the main text, the recursive simulation method approach amounts to computing a sequence of transition paths to a sequence of steady states that are consistent with a random walk assumption for the drivers. This approach is straightforward to implement in the Dynare package (Adjemian et al., 2011).

B.2 Calibration

We assume that households have different utility weights that apply between successive periods during three phases of life: 'young'; 'middle aged' and 'old'. These 'per-period' discount factors are denoted $\widetilde{\beta}_\tau$ and the utility weights in the model satisfy:

$$\beta_\tau = \prod_{s=1}^{\tau} \widetilde{\beta}_s \tag{B.1}$$

and our assumption that per-period discount factors vary by age implies that:

$$\widetilde{\beta}_\tau = \begin{cases} \widetilde{\beta}_Y & 1 \leq \tau < 5 \\ \widetilde{\beta}_M & 5 \leq \tau < 11 \\ \widetilde{\beta}_O & 11 \leq \tau \leq 14 \end{cases} \tag{B.2}$$

where $\widetilde{\beta}_Y$, $\widetilde{\beta}_M$ and $\widetilde{\beta}_O$ denote the per-period discount factors for young, middle-aged and old households respectively.

We choose the parameters $\widetilde{\beta}_Y$, $\widetilde{\beta}_M$ and $\widetilde{\beta}_O$ to best match two 'targets':

1. The real interest rate in the 1951–1955 steady state is close to the empirical estimate over the past (until 1950). Specifically, the target for the 1951–1955 steady-state annual real interest rate is 2%

(in line with the pre-1950 average of the empirical estimate, which is 1.93%).

2. The distribution of per capita assets $\{a_\tau\}_{\tau=1}^{T}$ matches a stylised distribution based on data on life-cycle asset holdings (see Lisack et al., 2021, for example). Specifically, the target per capita asset levels are 0.5, 1 and 0.75 for young, middle-aged and old households respectively.[33]

This is achieved by numerically minimizing a quadratic distance between the steady-state solution and the target. A weight of 10 is placed on matching the steady-state real interest rate and a weight of 1 is placed on matching the steady-state life-cycle asset distribution.

This process gives values for the discount factors of $\widetilde{\beta}_Y = 1.22$, $\widetilde{\beta}_M = 0.88$ and $\widetilde{\beta}_O = 1.72$.

B.3 Initial conditions

We implement a simple recursive approach to set the initial conditions for the simulation. The objective is to use data where available and otherwise to use steady-state relationships from the model.

1. Data for the drivers is used to set the initial conditions for $\left\{p_0^k, g_0, n_0\right\}$.
2. The empirical estimate of the equilibrium real interest rate in 1946–1950 is used to set r_0. We set r_0 consistent with an annual rate of 1.25%, close to the 1946–1950 average of the empirical estimate, which is 1.3%.
3. Population data for 1950 is used to directly set the initial conditions for the population shares in each cohort, $\{n_{\tau,0}\}_{\tau=1}^{T}$
4. Output, y_0, productivity growth, e_0, and labour force growth, l_0, are set equal to their 1951–1955 steady-state values.
5. Adjusted population shares, $\{m_{\tau,0}\}_{\tau=1}^{T}$ are set by 'inverting' the recursive laws of motion in the model:

$$
\begin{aligned}
m_{1,0} &= m_{1,1}\,(1+l_0)\,(1+n_0) \\
m_{\tau,0} &= \Pi_{\tau+1}^{-1}\,(1+l_0)\,m_{1,\tau+1}, \quad \tau = 2,\ldots,T
\end{aligned}
$$

   where $\{m_\tau\}_{\tau=1}^{T}$ are the adjusted population shares in 1951–1955 computed directly from the data. Setting the $\{m_{\tau,0}\}_{\tau=1}^{T}$ in this way ensures that the initial observed population structure is accurately captured in the simulation.
6. The initial capital stock k_0 is set by combining the capital to output ratio observed in the data with the assumption for initial output y_0 using the relationship:

$$
k_0 = s_{ky}\frac{y_0\,(1+l_0)\,(1+e_0)}{p_0^k}
$$

   where s_{ky} is the capital to output ratio in 1955, computed using the Penn World Table data for our sample of 31 countries.

B.4 Construction of the 'sensitivity swathe' (Figure 6)

We construct Figure 6 by replicating the recursive simulation under alternative assumptions about model parameter values and the paths of some drivers.

[33] We target the normalised levels (i.e., the *relative* sizes of asset holdings across cohorts).

For the model parameters, we consider the following sets of values (where the first element is our baseline assumption):

- $\theta \in \{1, 0.90, 1.1\}$
- $\sigma \in \{0.7, 1, 1.1\}$

For the cohort-specific (i.e., life-cycle) parameters ($\{\mathfrak{b}_\tau, \mathfrak{t}_\tau, \xi_\tau, \rho_\tau\}_{\tau=1}^{T}$) we consider two alternative assumptions:

- An equal allocation across all cohorts: $\mathfrak{b}_\tau = \mathfrak{t}_\tau = \xi_\tau = \rho_\tau = \frac{1}{T}, \tau = 1, \ldots, T$
- A distribution skewed towards older households: $\mathfrak{b}_\tau = \mathfrak{t}_\tau = \xi_\tau = \rho_\tau = 0, \tau = 1, \ldots, 9$; $\mathfrak{b}_\tau = \mathfrak{t}_\tau = \xi_\tau = \rho_\tau = 0.2, \tau = 10, \ldots, 14$

For the drivers (government debt to GDP, productivity growth, relative price of capital) we use alternative detrending assumptions, by considering two alternative values of λ in the filtering process: $\lambda = 100$ and $\lambda = 10,000$.

C Data

List of countries. Our sample comprises 31 'high-income' countries. A country is defined as high income if its output per capita in 2014 (computed as expenditure-side real GDP at current PPPs in mil. 2011US$ divided by total population from PWT9.0) is above 25,000$. From this list of countries, we remove oil-producing countries and 'fiscal paradises'.

The final list of countries is: Australia, Austria, Belgium, Canada, Czechia, Denmark, Estonia, Finland, France, Germany, Greece, Hong Kong, Hungary, Iceland, Ireland, Israel, Italy, Japan, Korea, Lithuania, Netherlands, New Zealand, Norway, Poland, Portugal, Singapore, Spain, Sweden, Switzerland, United Kingdom, United States.

C.1 OLG Model: Drivers

Population Growth
Description: Total population, both sexes combined, by five-year age groups. The growth rate of the population is the growth rate of the average size of the cohorts born in a given year between ages 20-64 (therefore the average is calculated across a diagonal of 9 observations).
Source: United Nations, Department of Economic and Social Affairs, Population Division (2017).
Aggregation: High-income aggregate.
Sample: 1950-2015.
Adjustments: Observations for the age buckets: '80-84', '85-89', '90-94', and '95-99' are not available before the year 1990, and instead there is one bucket, '80+'. Although these buckets are not used in the population growth calculation, following the 2018 methodology, these buckets are filled in before 1990 using the assumption that the weights assigned to each bucket within the '80+' category are the same as the first available observations for these more granular buckets (1990).

Survival Probability
Description: Total population, both sexes combined, by five-year age groups. The probability of survival is calculated by dividing the population of a certain five-year age group in a given five-year period by the previous (younger) five-year age group in the previous five year period.

Source: United Nations, Department of Economic and Social Affairs, Population Division (2017).
Aggregation: High-income aggregate.
Sample: 1950-2015.
Adjustments: We assume that the survival probability is 1 before age 65. Observations for the age buckets: '80-84', '85-89', '90-94', and '95-99' are not available before the year 1990, and instead there is one bucket, '80+'. For these observations, it is assumed that the percentage change in probability of survival in the year 2000 between each age bucket is the same previous to 2000. In this case the 5 year period ending in 1995 is also adjusted in this way, as it appeared to be an outlier. There is no observation for Π for the 5 year period ended 1955 due to the way that this variable is calculated based on population growth, therefore the probabilities are assumed to be the same as the next 5 year period ending in 1960.

Government debt to GDP ratio
Description: General government debt as a percent of GDP.
Source: Moreno Badia et al. (2018).
Aggregation: Cross-sectional weighted average of country-specific data with time-varying GDP weights from PWT (expenditure-side real GDP at current PPPs, in mil. 2017US$.
Sample: 1950-2017.

Labour-augmenting productivity
Description: Labour-augmenting technical change data (accounting for human capital) derived from a CES production function using data from Penn World Table 9.1.
Source: Ziesemer (2021).
Aggregation: Cross-sectional weighted average of country-specific data with time-varying GDP weights from PWT (expenditure-side real GDP at current PPPs, in mil. 2017US$.
Sample: 1950-2017.

Relative price of capital
Description: Ratio between the Price level of capital formation (`pl_i`) and the Price level of household consumption (`pl_c`).
Source: Penn World Table 10.0.
Aggregation: Cross-sectional weighted average of country-specific data with time-varying GDP weights from PWT (expenditure-side real GDP at current PPPs, in mil. 2017US$.
Sample: 1950-2019.

For each of the drivers described above, Figure C.1 plots the country-specific (where available) raw data together with its global trend component — i.e., after having (i) aggregated the data into a global concept using time-varying GDP weights and (ii) extracted the trend component as explained in Section 3.

Figure C.1 Structural Drivers: Raw Data & Common Trends

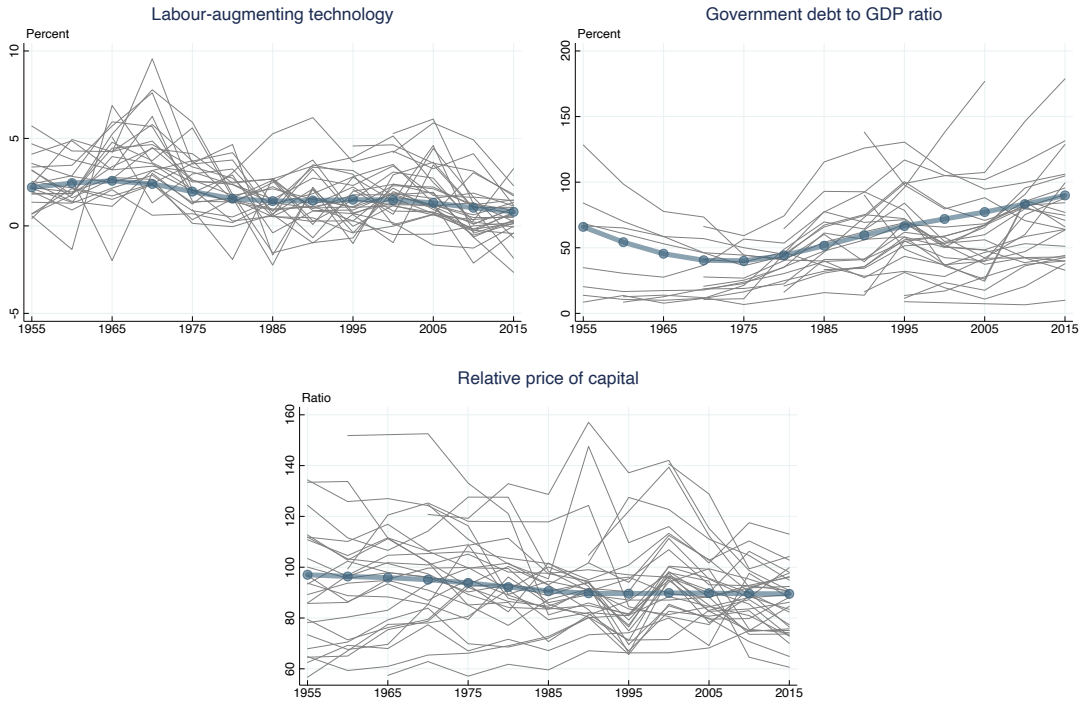

NOTE. The figure plots the raw data we use to construct the observable proxies for the exogenous processes that in the model drive changes in the global equilibrium real interest rate R^*. Grey lines plot country-specific data (where available), while the blue line with circles plots the common trend component of the raw data across countries. Sample period: five-year periods from 1955 to 2015, where 1955 corresponds to the period 1951-1955, see details in the text.

C.2 OLG Model: Data for Calibration

Real return on capital
Description: The real after-tax return to capital is constructed as total after-tax capital income, net of depreciation divided by the previous period's value of capital.
Source: Caballero et al. (2017).
Aggregation: US data.
Sample: 1955-2013.

Cohort-specific labour supply
Description: Civilian labour force participation rate by age.
Source: US Census (`https://www.census.gov/topics/employment/labor-force.html`).
Aggregation: US data.
Sample: Average across three data points 1996, 2006, and 2016. *Adjustments*: For the age buckets where the data was not as granular as we required, we assumed that the labour participation remained constant across those age groups. This is true for the cohorts '25-29' and '30-34' (as we have data only for the '25-34' cohort), '35-39' and '40-44', and '45-49' and '50-54'. For age buckets '80-84', '85-89', '90-94', and '95-99', labour participation rates are calculated by assuming a linear downwards trend between the rate in '75-79' (the oldest age group observed in the data) and zero participation for the age bucket '100+'.
Notes: We employ US data because of its superior granularity in the cross-sectional dimension (i.e., across cohorts). We cross-checked the patterns we obtain with US data with cross-country data from the OECD (which has information for only three cohorts, namely '15-24', '25-54', and '55-64'), and obtain very similar profiles for labour force participation.

Capital to output ratio
Description: Capital stock at constant 2017 national prices (in mil. 2017US$ divided by Real GDP at constant 2017 national prices (in mil. 2017US$).
Source: Penn World Table 10.0.
Aggregation: Cross-sectional weighted average of country-specific data with time-varying GDP weights from PWT (expenditure-side real GDP at current PPPs, in mil. 2017US$.
Sample: 1950-2019.

C.3 VAR Model: Observables

Short-term interest rates. *Description*: government bills or money market instruments. *Source*: Jorda et al. (2017) and Eikon Refinitiv. *Sample*: 1900-2017. *Aggregation*: Country-specific data.

Long-term interest rates. *Description*: government bonds. *Source*: Jorda et al. (2017) and Eikon Refinitiv. *Sample*: 1900-2017. *Aggregation*: Country-specific data.

Inflation rates. *Description*: Log-difference of CPI index. *Source*: Jorda et al. (2017) and Eikon Refinitiv. *Sample*: 1900-2017. *Aggregation*: Country-specific data.

Figure C.2 reports the real interest rates (measured as nominal rates minus inflation) for the 31 countries in our sample.

Figure C.2 Real Short-term Interest Rates Across Countries

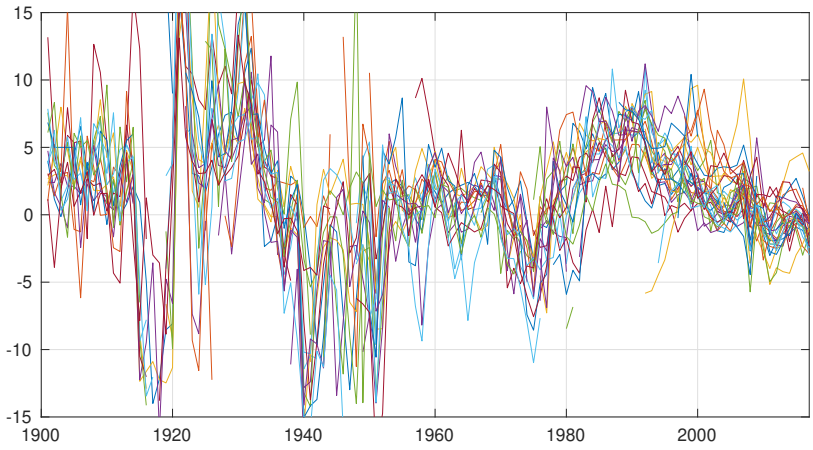

NOTE. Each line displays the short-term real interest rate, computed as the short-term nominal interest rate minus inflation, for a given country. The sample period runs from 1900 to 2017, where available (the panel is unbalanced).

D Estimating Global R^* Using a VAR with Common Trends

To obtain our empirical estimate of Global R^*, we use the approach developed by Del Negro et al. (2019), namely a vector autoregression (VAR) with common trends. The VAR allows to perform a multivariate trend-cycle decomposition and to extract the common trend component in real rates across countries. By imposing relatively uncontroversial restrictions on the long-run relations across variables (while remaining agnostic on whether these restrictions hold at shorter frequencies), we can interpret the estimated common trend in real interest rates across countries as the trend in the world real interest rate.

D.1 VAR Model

The VAR with common trends is based on Del Negro et al. (2017) and Del Negro et al. (2019), so this appendix closely follows the exposition in those papers. The model we estimate is a state-space model with measurement equation given by:

$$y_t = \Lambda \bar{y}_t + \tilde{y}_t \tag{D.1}$$

where y_t is an $n \times 1$ vector of observables; $\bar{y}_t$ is a $\tau \times 1$ vector of trends; $\tilde{y}_t$ is a $n \times 1$ vector of stationary components; Λ is a $n \times \tau$ matrix of loadings on which we impose restrictions based on economic theory (described below). The unobserved processes $\bar{y}_t$ and $\tilde{y}_t$ evolve according to a random walk and a VAR, respectively:

$$\bar{y}_t = \bar{y}_{t-1} + e_t \tag{D.2}$$

$$\tilde{y}_t = \sum_{l=1}^{p} \Phi_l \tilde{y}_{t-l} + \varepsilon_t \tag{D.3}$$

where Φ_l's are $n \times n$ matrices of coefficients. The $(\tau + n) \times 1$ vector of shocks $(e_t', \varepsilon_t')'$ is independently and identically distributed according to

$$\begin{pmatrix} e_t \\ \varepsilon_t \end{pmatrix} \sim \mathcal{N}\left(\begin{pmatrix} 0_\tau \\ 0_n \end{pmatrix}, \begin{pmatrix} \Sigma_e & 0 \\ 0 & \Sigma_\varepsilon \end{pmatrix} \right), \tag{D.4}$$

with the Σ's being conforming positive definite matrices, and where $\mathcal{N}(\cdot)$ denotes the multivariate Gaussian distribution. Equations (D.2) and (D.3) represent the transition equations in the state-space model. The initial conditions $\bar{y}_0$ and $\tilde{y}_{0:-p+1} = \left(\tilde{y}_0', \ldots, \tilde{y}_{-p+1}'\right)'$ are distributed according to

$$\bar{y}_0 \sim \mathcal{N}\left(\underline{y}_0, \underline{V}_0\right), \tilde{y}_{0:-p+1} \sim \mathcal{N}\left(0, V\left(\Phi, \Sigma_\varepsilon\right)\right), \tag{D.5}$$

where $V\left(\Phi, \Sigma_\varepsilon\right)$ is the unconditional variance of $\tilde{y}_{0:-p+1}$ implied by (D.3). The priors for the VAR coefficients $\Phi = (\Phi_1, \ldots, \Phi_p)'$ and the covariance matrices Σ_ε and Σ_e have standard form, namely

$$p\left(\varphi \mid \Sigma_\varepsilon\right) = \mathcal{N}\left(\text{vec}(\underline{\Phi})\Sigma_\varepsilon \otimes \underline{\Omega}\right)\mathcal{I}(\varphi) \tag{D.6}$$

$$p\left(\Sigma_\varepsilon\right) = \mathcal{IW}\left(\kappa_\varepsilon, \left(\kappa_\varepsilon + n + 1\right)\underline{\Sigma_\varepsilon}\right) \tag{D.7}$$

$$p\left(\Sigma_e\right) = \mathcal{IW}\left(\kappa_e, \left(\kappa_e + \tau + 1\right)\underline{\Sigma_e}\right), \tag{D.8}$$

where $\varphi = \text{vec}(\Phi), \mathcal{I}(\varphi)$ is an indicator function which is equal to zero if the VAR is explosive and to one otherwise, $\mathcal{IW}(\kappa, (\kappa + n + 1)\underline{\Sigma})$ denotes the inverse Wishart distribution with mode $\underline{\Sigma}$ and κ degrees of freedom. The prior for λ is given by $p(\lambda)$, the product of independent Gaussian distributions for each element of the vector λ.

D.2 Long-run Restrictions & Model Specification

Our baseline model includes data on the nominal yields of short-term (R_{it}) and long-term (R_{it}^L) government (or closely related) securities and inflation (π_{it}) for each of the 31 countries in our sample, where $i = 1, 2, ..., 31$ denotes a country. As in Del Negro et al. (2019) we extract a country-specific and a common trend for each of the observables. Specifically, we extract $(3 \times 31 + 3)$ trends from the cross-section of countries—a country-specific trend in inflation, the level of short-term interest rates, and the spread between long and short maturity rates; as well as a global trend in inflation, the level of short-term interest rates, and the spread between long and short maturity rates.

The key assumption imposed by Del Negro et al. (2019) to derive the long-run restrictions imposed on matrix Λ is the absence of arbitrage opportunities in the long run. In a simple asset-pricing framework, limits to arbitrage in the long-run imply the existence of a unique stochastic discount factor that prices all assets once their returns are exchange rate adjusted. Such unique stochastic discount factor, in turn, implies a common factor in country-specific interest rates, i.e. Global R^*.[34]

Specifically, the model we estimates is

$$R_{i,t} = \bar{r}_t^w + \bar{r}_t^i + \lambda_i^\pi \bar{\pi}_t^w + \bar{\pi}_t^i + \tilde{R}_{i,t}, \tag{D.9}$$

$$R_{i,t}^L = \bar{r}_t^w + \bar{r}_t^i + \overline{ts}_t^w + \overline{ts}_t^i + \lambda_i^\pi \bar{\pi}_t^w + \bar{\pi}_t^i + \tilde{R}_{i,t}^L, \tag{D.10}$$

$$\pi_{i,t} = \lambda_i^\pi \bar{\pi}_t^w + \bar{\pi}_t^i + \tilde{\pi}_{i,t}, \tag{D.11}$$

[34]The additional assumptions are that (i) the growth rate in the real exchange rate has no trend, a weaker than purchasing power parity in the long run; and (ii) the joint second moments of the variables that enter the Euler equations have no trend. See Del Negro et al. (2019) for more details.

for $i = 1, 2, ..., 31$, and where $\overline{R}_{it} - \overline{\pi}_{it} = \overline{r}_t^w + \overline{r}_t^i$; $\overline{\pi}_{it} = \lambda_i^\pi \overline{\pi}_t^w + \overline{\pi}_t^i$; and $R_{it}^L - R_{it} = \overline{ts}_t^w + \overline{ts}_t^i$. The system is estimated jointly for all 31 countries in the sample (so $n = 93$ and $\tau = 96$, as we have both global and country-specific trends).

D.3 Priors and Initial Conditions

As in Del Negro et al. (2019), the prior for the VAR parameters φ is a standard Minnesota prior with the hyperparameter for the overall tightness equal to the commonly used value of 0.2 (see Giannone et al., 2015). The only exception is the 'own-lag' parameter which is centered at zero rather than one. The prior for the covariance Σ_ε of the innovations to the cycles $\tilde{y}_t$, is a relatively diffuse inverse Wishart distribution with degrees of freedom ($\kappa_\varepsilon = n + 2$). The prior mean is set to be a diagonal matrix, with square root equal to 2, with the exception of the inflation cycle. Its prior mean is set to 4, to reflect the belief that nominal cycles might be more volatile than the other cycles.

We set the prior for Σ_e, the variance-covariance matrix of the innovations to all (common and country-specific) trends $\bar{y}_t$, to have a mode equal to a diagonal matrix with elements equal to 0.007 for all the real trends. This prior implies that the expected change in the trend over 100 years has a standard deviation equal to 0.7 percent. For the inflation trends, we use a value equal to 2×0.007, implying that the expected change in the trend over 50 years has a standard deviation equal to 0.7 percent. The degree of freedom is set to $\kappa_e = 400$.

We set the initial conditions to 4.7 percent for the real rate, 3.2 percent for inflation, and 0 percent for the term spread, in line with the sample averages over the period 1900 to 1920. As in Del Negro et al. (2019), the standard deviation for the initial conditions is set to 2 for the world inflation trend and 1 for all the others. The initial conditions for the country-specific trends have mean zero and standard deviations equal to half the value of the corresponding world counterparts.

All results are based on $5,000$ simulations, of which we discard the first $2,500$ as burn-in draws.[35]

D.4 Additional Results

This section provides additional results on our empirical estimate of Global R^*. A comparison with the original estimates by Del Negro et al. (2019) is reported in Figure D.1. The Figure shows that extending the model from 7 to 31 countries leads to a very similar posterior median, but allows us to obtain substantially more precise estimates of R^*, as shown by the narrower posterior coverage intervals. Figure D.2 reports the results from a robustness exercise where we estimate the baseline model with a looser prior: specifically, we use 200 instead of 400 degrees of freedom. The Figure shows that the estimated pattern of Global R^* is very similar across the two specifications. If anything, with a looser prior we obtain a slightly quicker and stronger pick up in R^*, which is more in line with the predictions from the model.

[35] The Gibbs sampler is described in Appendix A of Del Negro et al. (2017).

Figure D.1 Baseline R^* Estimate (31 countries) Vs. Del Negro et al. (2019) Estimate

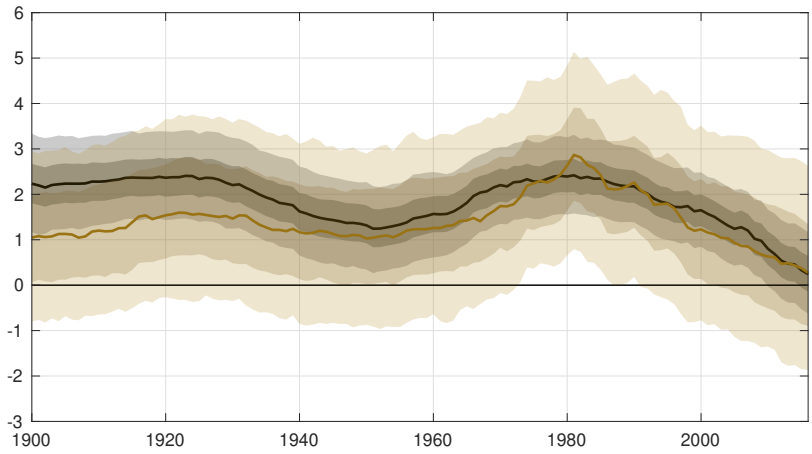

NOTE. The black line and shaded areas show the posterior median and the 68 and 95 percent posterior intervals of the empirical estimate of Global R^* presented in Appendix D and based on data for 31 countries. The yellow line and shaded areas display the estimates from the same model based on data for the G7 as in Del Negro et al. (2019).

Figure D.2 Robustness: R^* Estimate with $\kappa_e = 200$ degrees of freedom

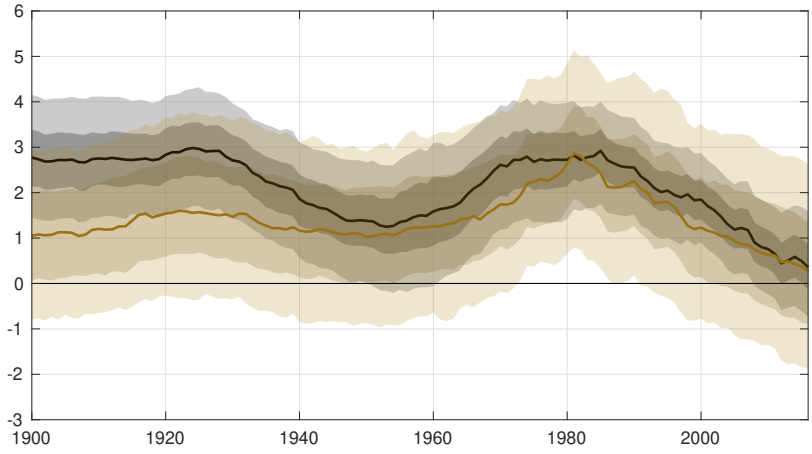

NOTE. The black line and shaded areas show the posterior median and the 68 and 95 percent posterior intervals of the empirical estimate of Global R^* presented in Appendix D and based on data for 31 countries with $\kappa_e = 200$ degrees of freedom. The yellow line and shaded areas display the estimates from the same model based on data for the G7 as in Del Negro et al. (2019).